npj | science of food

Article

Published in partnership with Beijing Technology and Business University & International Union of Food Science and Technology

https://doi.org/10.1038/s41538-025-00603-8

Effect of Pullulanase debranching freeze-thaw treatments and fatty acid on functional properties of yam starches

Ping-Hsiu Huang[1,6], Yu-Tsung Cheng[2,6], Wen-Chien Lu[3], Po-Yuan Chiang[4], Chin-Chuan Hsu[5], Chiun-Chuang R. Wang[5] & Po-Hsien Li[5] ✉

This study was performed using yam starches (Tainung No. (TNG)1 and 2), which were modification through Pullulanase debranching (PD) or addition of four fatty acids [lauric acid (LA), myristic acid (MA), palmitic acid (PA), and stearic acid (SA)], followed by one cycle of freeze-thaw synergy treatment. This study showed that increasing enzyme levels and extending treatment time during the PD synergized FT process significantly increased the amylose contents of yam starches from 33–36 to 48–65% ($p < 0.05$). Notably, the crystalline structure of yam starches changed from B to C-type, while those treated with fatty acids changed to C + V-type. This study showed that the glycemic index (eGI) of adding fatty acids to TNG2 starch treated with PD synergistic FT was consistent with the definition of low GI foods. Therefore, this study reveals techniques that can enhance yam starch's functional properties, which may interest food industry stakeholders.

Yam, a tuber crop, is known for its high mucilage and starch levels[1,2]. The starch contents of fresh yam ranges from 16 to 24%, while the dried bases contain 60 to 89% starch[1,3,4]. In Asia, Africa, South America, and the Caribbean, traditional medicine is vital for the prevention and treatment of diabetes and anemia, malaria treatment, and staple food, as well as for supporting the economies, food, and nutrition security of developing countries[1,2,5–8]. Despite extensive research on yam mucilage (polysaccharide) and steroidal saponins[2,3,9], the starch component of this plant species has remained largely underexplored[5]. This is probably due to the lack of value-added research on yam starch, which prevents it from attaining international commercial competitiveness[5]. It is worth considering that native yam starch exhibits lower water solubility, temperature intolerance, and susceptibility to gelatinization[10]. Another possibility is that yams were primarily utilized as fresh food, vegetables, and herbs in the past[4,11], with only a limited number of processed food applications.

Starch, a microcrystalline polymer composed mainly of amylose and amylopectin with unique physicochemical properties, is used in various industrial sectors and serves as a valuable energy source and functional ingredient[12–14]. Following the PD process, starch undergoes enzymatic cleavage of its α-1,6 glycosidic bonds to produce a mixture of long and short unit chains. This unique property enables the formation of resistant starch (RS), which is widely utilized in various industries[15–17]. More specifically, these modified processes are particularly favored for producing RS, slowly digested starch (SDS), maltose, dextrins, glucose syrup, oligosaccharides, fat substitutes, adhesive products, corrugated boards, cardboard boxes, and paper[18–23]. This broad range of applications is attributed to the exceptional functionality of these modified starches. The increasing demand for modified starches is a testament to their versatility and effectiveness in enhancing product quality and performance. The drawbacks of the traditional method of starch modification are challenging to overcome, such as the high temperature required for gelatinization, retrogradation, insolubility, weak mechanical features, and unusual viscosity[13,24–26]. To mitigate these issues, it is crucial to explore innovative techniques, such as the synergistic utilization of distinct approaches, including the dual modification of starches. This approach has created more functionalities, such as stable hydrocolloids, RS, and films[18,19,27–29]. A feasibility methodology must be comprehensively developed to identify potential capacities and pave the way for practical implementation.

This study investigated the physicochemical properties of TNG1 and 2, two yam starches. This will be achieved through the PD synergistic FT 1-cycle dual modification treatment and adding fatty acids with different processing techniques. This study aimed to provide a more in-depth understanding of the changes in the properties above and their impact on the final product. In this study, we investigated the changes in the contents of

[1]Department of Food Sciences, National Chiayi University, Chia-Yi City, Taiwan. [2]Cardiovascular Center, Taichung Veterans General Hospital, Taichung City, Taiwan. [3]Department of Food and Beverage Management, Chung-Jen Junior College of Nursing, Health Sciences and Management, Chia-Yi City, Taiwan. [4]Department of Food Science and Biotechnology, National Chung Hsing University, Taichung City, Taiwan. [5]Department of Food and Nutrition, Providence University, Taichung City, Taiwan. [6]These authors contributed equally: Ping-Hsiu Huang, Yu-Tsung Cheng. ✉e-mail: pohsien0105@pu.edu.tw

RS, SDS, and rapidly digested starch (RDS), including modified yam starch with its digestibility and estimated glycemic index (eGI). In addition, this study also examined the molecular weight (MW) distribution, structure, relative crystallinity (RC), thermal, and pasting properties. The findings of this study were expected to serve as a significant reference point for researchers in the development of RS or low-GI foods, paving the way for innovative research and development in this field.

Results and discussion

Amylose content

This study revealed that gelatinization (100 °C, 1 h) of TNG1 and 2 resulted in approximately 5.53–5.94% of amylose content following pasting (Table 1). The observed amylose content reduction in the starch solution is attributed to the structural modification of the starch, which occurs because of gelatinization due to heating. Following gelatinization, PD, and FT 1 cycle treatments, there was a slight increase in amylose content, ranging from 7.87 to 9.90%. Based on the available data, FT treatment positively impacts the recrystallization of the intermolecular double helix structure. Consequently, this leads to an improvement in amylose content. However, during PD with different enzyme activities (8, 12, 16, 20, and 24U) treated for 24 h, there was a discernible relationship between the enzyme activities and amylose contents in pasted yam starches TNG1 and 2. Specifically, the amylose content increased from native levels of 33–36% to approximately 40–50% ($p < 0.05$). Notably, the amylose contents of TNG1 and 2 consistently increased as the PD time progressed to 40 h, ultimately reaching a range of 48–65%, and there were significant differences for each group ($p < 0.05$). According to a report by Shi and Gao[30], it was observed that treatment with pullulanase resulted in a significant increase in the amylose content of glutinous rice starch, while the observed increase ranged from 21–30%. The research conducted by Tu et al.[31] found that extensive debranching of lotus seed amylopectin using 8–10 FT treatments increased amylose content. Simultaneously, amylose single helices in starch undergo recrystallization and rearrangement, contributing to a decrease in the hydrophilicity of starch, namely, weakening of the aggregation interactions within the starch granules[31]. However, it has been reported that FT treatment decreases the amylose contents of potatoes[32], pumpkin[33], and wheat starches[34]. In particular, the decomposition of amylose into shorter ones, with an accompanying tendency for increased proportions of amylopectin[32]. Therefore, during the process of starch retrogradation, the starch molecules aggregated into double-helix form through hydrogen bonding and van der Waals force to form a three-dimensional (3D) network structure[35]; namely, the higher the content of amylose, the starch is easier to age and reduce the rate of hydrolysis of starch, which is beneficial to lowering glycemic and insulin responses[33].

MW distribution

The findings of this study, as determined by GPC, reveal that the compositions of native TNG1 and 2 starches exhibit a higher proportion of macromolecule components, with a lesser portion composed of small ones (Fig. 1A and B). At the same time, it was predicted that following the gelatinization process, the macromolecular structures of both TNG1 and 2 starches had a lower distribution. This can be attributed to the alteration of the starch structure by heat. However, the TNG1 and 2 starches underwent gelatinization (100 °C, 1 h), followed by PD treatment utilizing different enzyme activities (8–24U). The results of this study revealed an increase in the distribution of small MW components, with a positive correlation between enzyme activity and treatment time, with the trend reported by Zhang et al.[36]. The conversion of long amylopectin molecules into shorter amylopectin or amylose molecules with a smaller MW can be attributed to pullulanase hydrolysis of the α-1, 6-glycosidic bonds in amylopectin, which reduces the double helix structure of amylopectin, ultimately damaging the crystalline structure of starch[37,38]. This enzyme can cleave larger molecules of long amylopectin, breaking them down into smaller forms[12,39]. Notably, starch gelatinization followed by PD leads to the hydrolysis of long amylopectin into shorter ones, contributing to the formation of RS[40]. However, this phenomenon in PD treatments has been found to cause an increase in RDS and a decrease in RS in starch-based products[12]. Tu et al.[31] reported that increasing the frequency of FT treatment cycles facilitated the continued smaller size of lotus seed starch particles. Simultaneously, the same authors also suggested that aggregation of the lotus seed starch particles in the aqueous phase interrupts the MW-decreasing interaction due to the formation of complexes with lipids.

RDS, SDS, and RS contents

Starch digestibility is influenced by various factors, including but not limited to the source, composition, size, production process, cooking method, and chewing level[41,42]. Enzymatic, physical, or chemical modifications approaches or genetic modifications can increase starch properties and SDS content, thereby delaying the digestibility of starch in the gastrointestinal tract[43]. It is important to note that starch digestibility is a complex process subject to multiple variables that must be carefully considered in research studies and industrial applications. In addition, it is essential to consider the RS type and food processing method to measure the RS content and formulate dietary recommendations[42]. This consideration ensured the accuracy and precision of the results.

The findings of this study revealed the RDS and SDS contents of two varieties of yam starch, TNG1 and 2, post-gelatinization (100 °C, 1 h). The RDS contents of TNG1 and 2 were 35.63 and 33.32%, respectively, while the SDS contents were 39.73 and 35.91%, respectively (Table 1). Moreover, for the TNG1 and 2 starches, following the sequential treatment of the starch paste with PT and FT for one cycle, it was observed that there was a decrease in the RDS content to a range of 19–20% and a slight increase in the SDS content from 42.68 to 40.97%. Starch pasting is a process in which the crystalline structure of starch is broken down by exposure to high temperatures[44]. This results in improved digestibility of starch and alterations in the composition of RDS and SDS[45].

Moreover, the TNG1 and 2 starches underwent gelatinization and were subsequently treated with varying levels of the PD synergized FT 1 cycle. The RDS content remained lower than those in the gelatinized and retrograded groups. With increasing in PD treatment time, the difference in RDS content was reduced, and there were significant differences between all groups ($p < 0.05$). According to Miao et al.[46], waxy maize starch is slowly digested because of the tight amorphous regions in the dual helices of starch granule crystallites that develop from imperfect reorganization during gelatinization and retrogradation. The authors mentioned above reported that treating starch with 20 or 40 ASPU/g of PD for more than 6 h led to a decrease in SDS and an increase in RS content. Moreover, they found a negative correlation with the RDS content. This study was unsuccessful in identifying any discernible trends, which may be due to the disparities in the starch content and treatment. However, FT treatment may also cause starch retrogradation, thereby decreasing RDS content. This study showed that lower SDS content could be maintained by utilizing appropriate PD levels (16 and 20 U for TNG1, 16–24 U for TNG2) and synergizing the FT 1 cycle treatment. These connections were found to be significantly different ($p < 0.05$) from those of the others. In addition, Tu et al.[31] reported that PD treatment synergized with FT treatment for 6–10 cycles during the modification period, and the RDS in lotus seed starch decreased consistently, whereas SDS and RS increased, indicating that the formation of V-type starch proved to be resistant to digestive enzymes. At the same time, these results echoed the XRD results of this study[31,47]. Therefore, PD treatment in cooperation with FT treatment helps protect starch granules against the effects of digestive enzymes, and this structure is stabilized by hydrogen bonding, leading to the formation of RS[48]. Afterward, post-paste TNG1 and 2 starches were subjected to different levels of PD, followed by the addition of the four types of fatty acids (LA, MA, PA, and SA), and then by the FT 1 cycle. The RDS contents of TNG1 and 2 were 16–19 and 12–17%, respectively (Table 1), while the SDS contents were 25–34 and 22–25%, respectively. However, the values shown were not significantly different from the results for the non-added fatty acid groups. Notably, the inclusion of SA effectively reduced the SDS content, comparable to the PD mentioned above in the treatments.

https://doi.org/10.1038/s41538-025-00603-8

Table 1 | Effects of amylose, rapidly digestible starch (RDS), slowly digestible starch (SDS), resistant starch (RS) contents via Pullulanase debranching (PD; 40 h), synergized freeze-thaw (FT) treatment, and four fatty acids' addition on the two yam varieties starches

Yam varieties	Status		Amylose content (%)			Total starch	Rapidly digestible starch (RDS)	Slowly digestible starch (SDS)	Resistant starch (RS)
			0[1]	24	40	0	40	40	40
Tainung No.1 (TNG1)	Native starch		36.37 ± 0.91^{a}	-		79.8	7.59 ± 3.07^{cd}	7.34 ± 0.66>^{g}	64.70 ± 0.03^{a}
	Gelatinize starch[2]		5.94 ± 0.28^{d}			-	35.63 ± 1.10^{b}	39.73 ± 2.05^{a}	5.40 ± 0.00^{i}
	Retrograde starch[3]		7.87 ± 0.19^{e}				19.45 ± 0.41^{d}	42.68 ± 0.49^{g}	17.70 ± 0.01^{b}
	Pullulanase debranching (PD) synergized freeze-thaw (FT) 1-cycle	8U[4]	-[6]	40.41 ± 0.92^{d}	49.68 ± 0.89^{d}		13.11 ± 1.84^{b}	38.13 ± 2.10^{a}	29.60 ± 0.04^{i}
		12U		43.54 ± 0.44^{cd}	49.94 ± 0.95^{d}		16.73 ± 0.49^{a}	32.77 ± 3.26^{abc}	32.30 ± 0.02^{h}
		16U		45.21 ± 0.34^{c}	52.04 ± 1.12^{e}		11.53 ± 0.68^{a}	29.27 ± 1.98^{abcd}	39.00 ± 0.01^{h}
		20U		49.51 ± 0.16^{b}	58.83 ± 3.58^{a}		15.41 ± 1.49^{bcd}	29.89 ± 2.47^{a}	40.80 ± 0.05^{d}
		24U		47.53 ± 0.48^{b}	64.01 ± 2.16^{e}		17.17 ± 0.98^{bcd}	32.36 ± 2.49^{abcdef}	33.30 ± 0.03^{c}
	Lipid	LA[5]	-				16.89 ± 0.42^{bc}	34.94 ± 0.50^{f}	27.97 ± 0.50^{g}
		PA					18.46 ± 0.66^{a}	29.40 ± 0.34^{abc}	31.93 ± 0.98^{c}
		MA					19.07 ± 0.93^{a}	28.13 ± 0.60^{bcd}	33.10 ± 1.15^{d}
		SA					16.73 ± 0.35^{bcd}	25.20 ± 0.18^{abc}	37.87 ± 0.40^{e}
Tainung No.2 (TNG2)	Native starch		33.13 ± 0.59^{b}	-		75.1	8.26 ± 2.09^{bcd}	5.47 ± 1.59^{def}	61.4 ± 0.03^{de}
	Gelatinize starch		5.53 ± 0.29^{c}			-	33.32 ± 3.19^{bcd}	35.91 ± 3.08^{def}	5.90 ± 0.00^{d}
	Retrograde starch		9.90 ± 0.13^{e}				20.19 ± 0.92^{bc}	42.05 ± 1.68^{abcde}	14.40 ± 0.01^{d}
	PD synergized FT 1-cycle	8	-	41.53 ± 0.48^{a}	48.39 ± 0.61^{b}		14.13 ± 2.88^{bcd}	35.83 ± 2.53^{ab}	25.20 ± 0.04^{de}
		12		44.13 ± 0.13^{c}	50.38 ± 0.28^{d}		14.39 ± 2.42^{bcd}	33.88 ± 0.72^{abcde}	33.40 ± 0.08^{ef}
		16		47.68 ± 0.42^{b}	63.83 ± 1.30^{c}		15.60 ± 2.56^{bcd}	23.96 ± 3.11^{f}	39.50 ± 0.02^{d}
		20		50.67 ± 0.64^{a}	65.72 ± 2.12^{e}		13.11 ± 1.31^{bcd}	27.40 ± 5.03^{ef}	44.90 ± 0.09^{g}
		24		48.91 ± 0.91^{ab}	65.38 ± 0.84^{e}		17.87 ± 1.34^{bcd}	26.50 ± 1.67^{cdef}	24.00 ± 0.0^{fg}
	Lipid	LA	-				17.53 ± 0.58^{bcd}	25.97 ± 1.08^{de}	31.60 ± 0.92^{f}
		PA					16.11 ± 0.35^{bcd}	25.99 ± 0.30^{de}	30.73 ± 1.63^{f}
		MA					13.59 ± 0.22^{bcd}	26.31 ± 0.48^{de}	35.21 ± 0.26^{f}
		SA					12.92 ± 0.40^{bcd}	22.68 ± 0.55^{e}	39.51 ± 0.56^{f}

[1] Pullulanase debranching (PD) treated time (h).
[2] Gelatinize starch: native starch is heated in boiling water (100 °C) for 1 h.
[3] Retrograde starch: freeze-thawing 1 cycle for 24 h.
[4] Pullulanase activity (U/g starch).
[5] Lauric acid (LA; C12); Myristic acid (MA; C14), Palmitic acid (PA; C16), and Stearic acid (SA; C18).
[6] Not measured.
Different lowercase letters labeled in the same column represent significant differences ($p < 0.05$).

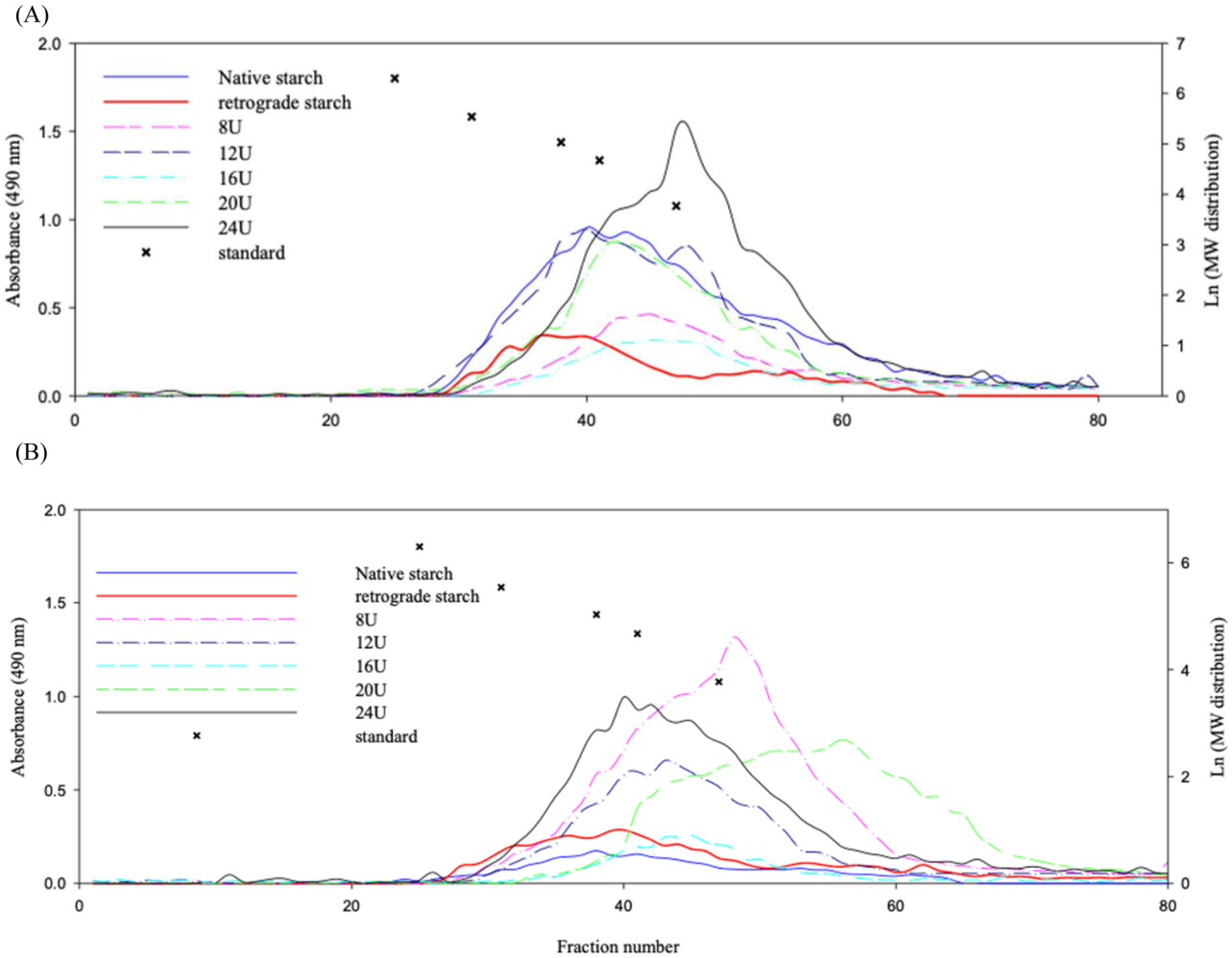

Fig. 1 | Molecule weights of starch treated with Pullulanase debranching (PD) synergized freeze-thaw (FT). A Tainung No.1 (TNG1) and **B** Tainung No.2 (TNG2).

However, the absence of a significant increase in SDS can be attributed to the formation of amylose-lipid complexes. It is worth noting that ascorbyl palmitate added to native potato starch and high-amylose maize starch was found to increase RS type 5 (RS5; self-assembled starch-lipid inclusion complex)[49] and decrease SDS and RDS contents due to complex formation, according to Guo and Kong[50]. The authors also concluded that the addition of PA had no significant inhibitory effect. Moreover, PD treatment can result in the formation of short amylose and broken amylopectin substances within starch. Alternatively, adding fatty acids to the mix can form a double-helix structure with amylose, allowing for re-condensation of the starch. It is essential to note that such a structure is often incomplete, resulting in a starch crystalline structure that is less dense and therefore slower to digest[51]. Notably, Guo et al.[42] reported that the contribution of the RS type 3 (RS3) should also be considered alongside discussing the practical, beneficial effects of the RS5.

The RS content of native TNG1 and 2 yam starches was 64.7% and 61.4%, respectively. However, the RS content decreased to 5.40 and 5.90% in gelatinized (100 °C, 1 h) TNG1 and 2 yam starches, respectively. The observed phenomena can be attributed to the rupture of starch particles in the yam and the reduction in RS content due to the high temperatures. Furthermore, there was a decrease in the double-helix structure of the starch molecules. In addition, Pongjanta et al.[52] reported that rice starch (moisture content of approximately 15%) was treated with pullulanase followed by placing the starch paste at 4, −10, and 30 °C for 16 h each. The starch undergoes retrogradation to enhance the RS content, while the trend was similar to the results of this study. Bodjrenou et al.[12] found that extending the treatment time of purple sweet potato starch with PD from 5 to 20 h, followed by retrogradation at 4 °C for 24 h, and increased the yield of RS. However, extending the PD treatment beyond 20 h showed the opposite effect. The authors also suggested amylopectin production from fewer short, linear molecules, followed by retrogradation and rearrangement into new crystal structures. Interestingly, the RS contents of TNG1 and 2 yam starches underwent a substantial increase, ranging from 24.0–44.9%, following PD synergized FT 1 cycle treatments. This result indicates the potential efficacy of utilizing PD synergized FT 1 cycle treatments to increase the RS content of yam starch. PD 16 and 20U treatments followed by the FT 1 cycle treatment exhibited the highest contents, and there were significant differences ($p < 0.05$) compared to the other groups. Liu et al.[40] reported that waxy maize starch with PD treatment enhanced RS content from 13 to 19%, attributable to increased amylose content, which was similar to this study's results. In addition, the RS content of the groups that were PD-treated for 40 h, followed by the addition of fatty acids, and then FT treatment ranged from 29.0 to 40.0% (TNG1) and from 12.0 to 39.5% (TNG2) (Table 1). In particular, the SA-supplemented group exhibited the highest RS content, which was significantly different from the other groups. However, there were insignificant differences in the RS content compared to those without the addition of fatty acids, and the trends were similar to the changes in SDS content described above. This study indicated that the group that received SA had similar outcomes to those treated with PD (16 and 20U). Glucan chains with a degree of polymerization (DP) equal to or less than 10 encounter difficulties in forming crystalline structures, resulting in low RS content[53]. Specifically, short linear chains with DP ≤ 13 can be conducive to a favorable chain rearrangement, resulting in a well-structured RS crystal with double helices that enhance alignment, molecular mobility, and

aggregation[51,54]. However, Zhang et al.[55] reported that amylase mainly disrupts the amorphous regions of the starch during gastric digestion. Meanwhile, an increase in DP > 30 chains promotes the rearrangement of single- and double-helix starch structures. Moreover, as intestinal digestion continues, the starch's single helix and amorphous content decrease with the digestion duration[55]. In addition, the physicochemical properties of the starch, including particle size, composition, and specific surface area, also influenced digestibility[56]. The yield of gelatinization PD synergistic FT-modified TNG1 and 2 yams' RS was contingent upon the conditions applied to the modifications. Therefore, it may be associated with the molecular quality and distribution[15], necessitating further investigations.

Thermal properties

This study showed that the gelatinization temperatures (To, Tp, Tc) and ΔH of two native yam starches (TNG1 and 2) were significantly reduced by FT 1 cycle treatment (Table 2). It was assumed that this could be attributed to the destruction of the double helix structure of partial starch molecules in the crystalline region of the starch during the gelatinization process. Subsequently, starch retrogradation occurred after the FT 1 cycle treatment, which resulted in lower pasting temperatures and ΔH values of the pasted starch[57]. However, the gelatinization temperatures of the pasted yam starches treated with the PD synergized FT 1 cycle showed a decreasing trend ($p < 0.05$) compared with the native group. The PD 24U group showed the smallest decrease, being closest to the native group. Furthermore, it is worth noting that the ΔH change of all groups subjected to treatment with PD synergized FT 1 cycle exhibited a significant decrease, and the difference between the groups was also significant ($p < 0.05$). Again, the PD 24U group showed a minimum change in ΔH. On the other hand, higher pullulanase activity had fewer effects on the gelatinization temperature and ΔH compared to the native group. These phenomena can be attributed to the starch pasting process resulting in more debranching reactions, that is, more amylose is released or the formation of more short chains and branching points with higher enzyme activity[54,58]. According to several reports, FT treatment increases the gelatinization temperature of starch, which is associated with amylose recrystallization[59,60]. The reduction in ΔH during the pasting process is closely associated with the proportion of double helix structures in the crystalline and amorphous regions of the starch particles[57,61]. It has been reported that a decrease in ΔH results from the reduction of double helices in the amylose structure rather than a decrease in crystallinity[46]. Wang et al.[56] also reported that wet heat treatment promotes the formation of starch-lipid complexes and restricts the mobility of starch chains in the amorphous region. Meanwhile, the decrease in ΔH can be ascribed to the fact that the high temperature disrupts the hydrogen bonding in the crystalline region of the starch[56]. Furthermore, FT treatment has been reported to increase the gelatinization temperature of potato starch while contributing to the formation of a more ordered and compact crystalline structural region[32]. Simultaneously, FT-treated potato starch contained high levels of amylopectin, forming a stable structure that led to a larger ΔH[32,62]. This phenomenon has also been reported in the dough of steamed buns, where an increase in the frequency of FT treatment cycles revealed an increasing trend in ΔH[63]. In practical applications, it is important to carefully consider the intricate processes of molecular rearrangement and self-assembly with modifications in the starch[64]. Low and Liao[65] also reported that the nutritional function of starch could be altered by adding emulsifiers to the formulation, which also formed a V-type crystalline structure with starch, thereby enhancing its digestive resistance.

Moreover, this study revealed that including fatty acids led to a significant increase in gelatinization temperatures, which were significantly different ($p < 0.05$) from those of the groups without such addition. In addition, the thermal properties of the SA-added group were comparable to those of the PD24U group. This also indicates that an increase in gelatinization temperature can be attributed to amylose and lipid recrystallization during the pasting process[66]. It was postulated that the formation of complexes between the amylose double helix and various fatty acids, such as LA, PA, MA, and SA, may explain the observed changes in the gelatinization temperature. Moreover, this phenomenon also occurred at another peak at high temperatures; specifically, Peak I appeared between 52 to 70 °C, while Peak II occurred at over 90 °C. Peak I was arranged in a more structured form, resulting in lower gelatinization temperatures, whereas Peak II was a polycrystalline compound with higher gelatinization temperatures[67]. It was hypothesized that this could be due to the effects of the melting point of the free fatty acids[36,68]. The phenomenon has been attributed to the formation of single amylose helices and lipid complexes[69,70]. The occupancy of starch helix cavities by fatty acids is believed to render the starch system stable in a low ΔH state[69,70]. This stability effectively prevents starch from being disturbed by external factors[69].

Paste properties

The findings of this study suggest a drastic decrease in the pasting properties of yam starch that underwent PD synergized FT treatment (TNG1 and 2) compared to native and retrograde starches (Fig. 2). All parameters (Table 3) exhibited statistically significant differences among all groups ($p < 0.05$). Shen et al.[32] reported that FT-treated starches can be affected by a decreased ratio of amylose to amylopectin in the pasting properties. The same authors reported that potato starches have higher pasting temperatures, troughs, and final viscosities, with the opposite trend observed for the breakdown and setback viscosities. However, the variation in the pasting properties of yam starch in this study could not be explained by compositional changes in starch. Yam starch was pasted in this study, followed by the PD synergized FT 1 cycle treatments. Moreover, the temperature at which pasting occurred demonstrated a positive correlation with the level of enzyme activity, peaking at the highest point in the 24U + FT group (Table 3). It was hypothesized that the possible reasons might be attributed to the PD synergized FT treatments altering the structure of the yam starch with dose-dependent enzymatic activity. This phenomenon is attributed to the limited capacity of starch to absorb water, resulting in decreased swelling[71]. Another possible explanation is that the gelatinization process (100 °C, 1 h) and PD synergized FT treatments employed during preparation could have contributed to the reduced gelatinizing capacity of yam starches. This observation has also been noted in other published studies[15,72]. Moreover, the same results as above were presented regarding incorporating different fatty acid modifications; namely, all parameters of the pasting properties showed dramatic decreases. However, further studies are needed regarding the application of modified yam starch in food products in this study.

Granules morphology

The SEM results of this study revealed that the native yam starch (TNG1 and 2) had round and elliptical shapes with smooth surfaces (Fig. 3). Meanwhile, the retrograde starches that underwent gelatinization (100 °C, 1 h) and FT 1 cycle treatment starches with intact particles lost their complete structure owing to high-temperature pasting and exhibited a continuous and smooth structure. This phenomenon results from the absorption of adequate quantities of water by starch particles and the attainment of pasting temperature[73]. Subsequently, the starch particles rupture and connect with the neighboring ruptured particles, forming a smooth structure[74]. Moreover, since recrystallization and freeze-shrinkage occur during FT, rearrangement of the starch structure occurs and decreased separation of interstitial regions of proteins from neighboring ice crystals, contributing to mechanical damage to the microstructure[75]. During retrogradation, starch particles tend to get closer to each other because of the formation of hydrogen bonds, leading to the generation of nuclei and the formation of large-sized crystals post-expansion[15]. However, the yam starches that underwent treatment with PT synergized with FT, revealing the presence of tiny pores on the surface of starch granules (Fig. 3C–G and J–N). The number of these pores may be positively correlated with enhanced enzyme activity[76]. It is worth mentioning that Li et al.[54] reported that the rice starch particles might be insensitive to PD, and no pores were evident on the surface of the starch particles post-PD treatment. Bodjrenou et al.[12] have also reported that PD treatment, sterilization, and retrogradation altered the starch particle structure; namely, the surface of the starch particles formed rough,

https://doi.org/10.1038/s41538-025-00603-8

Table 2 | Effects of thermal properties via Pullulanase debranching (PD; 40 h), synergized freeze-thaw (FT) treatment, and four fatty acids' addition on the two yam varieties starches

Yam varieties	Status		Peak I				Peak II			
			Temperature (°C)			Paste enthalpy (J/g)	Temperature (°C)			Paste enthalpy (J/g)
			onset (To)	peak (Tp)	end (Tc)	ΔH	To	Tp	Tc	ΔH
Tainung No.1 (TNG1)	Native starch		71.38 ± 1.23^{b}	74.36 ± 3.02^{c}	78.84 ± 3.02^{b}	17.36 ± 0.14^{a}				
	Retrograde starch[1]		48.59 ± 1.02^{h}	58.47 ± 2.07^{h}	70.60 ± 2.14^{e}	8.17 ± 0.25^{c}				
	Pullulanase debranching (PD) synergized freeze-thaw (FT) 1-cycle	8U[2]	63.10 ± 2.03^{e}	64.74 ± 0.85^{f}	68.07 ± 1.46^{ef}	4.61 ± 0.31^{f}				
		12U	48.60 ± 1.14^{j}	53.81 ± 1.63^{i}	62.4 ± 1.32^{f}	1.10 ± 0.12^{gf}				
		16U	56.03 ± 1.25^{f}	72.67 ± 2.12^{d}	87.85 ± 1.25^{b}	3.96 ± 0.13^{d}				
		20U	46.96 ± 1.12^{hi}	53.97 ± 1.26^{i}	66.35 ± 2.02^{f}	4.26 ± 0.14^{de}				
		24U	68.64 ± 2.04^{c}	77.89 ± 1.59^{a}	83.66 ± 3.01^{b}	6.66 ± 0.17^{g}				
	Lipid	LA[3]	53.13 ± 1.03^{f}	66.40 ± 2.33^{c}	86.36 ± 3.22^{f}	0.93 ± 0.19^{d}	-			
		PA	57.99 ± 2.12^{f}	61.37 ± 3.29^{de}	66.01 ± 2.33^{e}	0.74 ± 0.25^{e}	96.28 ± 4.07^{a}	101.96 ± 3.64^{bc}	106.06 ± 3.25^{b}	0.56 ± 0.08^{d}
		MA	67.83 ± 1.07^{d}	68.72 ± 1.25^{b}	71.70 ± 3.26^{f}	0.80 ± 0.22^{ef}	100.21 ± 3.25^{a}	104.48 ± 2.53^{bc}	107.93 ± 4.12^{b}	1.46 ± 0.11^{c}
		SA	67.67 ± 2.05^{d}	68.66 ± 1.36^{b}	70.44 ± 3.27^{d}	0.35 ± 0.26^{ef}	97.32 ± 3.58^{a}	104.64 ± 1.94^{ab}	109.55 ± 3.22^{a}	1.67 ± 0.14^{b}
Tainung No.2 (TNG2)	Native starch		73.66 ± 1.58^{a}	76.66 ± 2.11^{b}	80.54 ± 3.12^{c}	17.80 ± 0.24^{a}				
	Retrograde starch		48.50 ± 1.68-^{gh}	59.94 ± 1.35^{g}	76.94 ± 3.05^{d}	11.49 ± 0.2-1^{b}				
	PD synergized FT 1-cycle	8	66.31 ± 2.44^{d}	78.34 ± 2.27^{a}	92.10 ± 3.11^{a}	2.30 ± 0.27^{ef}				
		12	57.81 ± 1.14^{f}	69.08 ± 1.59^{e}	87.32 ± 2.02^{b}	4.41 ± 0.29^{de}				
		16	71.19 ± 2.05^{b}	73.82 ± 1.68^{c}	85.79 ± 2.36^{b}	1.02 ± 0.09^{g}				
		20	62.93 ± 1.38^{e}	78.18 ± 2.02^{ab}	88.76 ± 2.24^{b}	2.65 ± 0.07^{ef}				
		24	50.52 ± 1.42^{g}	53.67 ± 1.94^{i}	62.65 ± 2.15^{g}	0.94 ± 0.02^{ef}				
	Lipid	LA	60.45 ± 2.13^{e}	64.96 ± 1.88^{cd}	60.45 ± 2.02^{e}	0.11 ± 0.01^{ef}	93.40 ± 4.01^{b}	98.53 ± 3.57^{d}	102.53 ± 3.69^{c}	0.75 ± 0.07^{d}
		PA	60.38 ± 1.39^{e}	61.68 ± 1.67^{de}	63.65 ± 2.13^{e}	0.69 ± 0.02^{ef}	95.76 ± 3.85^{ab}	104.14 ± 4.26^{abe}	108.96 ± 4.02^{a}	2.13 ± 0.13^{a}
		MA	52.17 ± 1.85^{g}	53.16 ± 1.25^{g}	54.79 ± 2.36^{g}	0.06 ± 0.01^{f}	96.5 ± 3.42^{a}	101.96 ± 4.17^{c}	105.79 ± 3.25^{b}	1.60 ± 0.12^{bc}
		SA	70.44 ± 1.46^{c}	71.18 ± 1.34^{b}	73.75 ± 1.25^{c}	4.84 ± 0.14^{d}	97.3 ± 2.75^{a}	105.99 ± 4.36^{a}	111.09 ± 4.12^{a}	1.94 ± 0.17^{a}

[1] Retrograde starch: freeze-thawing 1 cycle for 24 h

[2] Pullulanase activity (U/g starch)

[3] Lauric acid (LA; C12); Myristic acid (MA; C14), Palmitic acid (PA; C16), and Stearic acid (SA; C18).

Different lowercase letters labeled in the same row represent significant differences ($p < 0.05$).

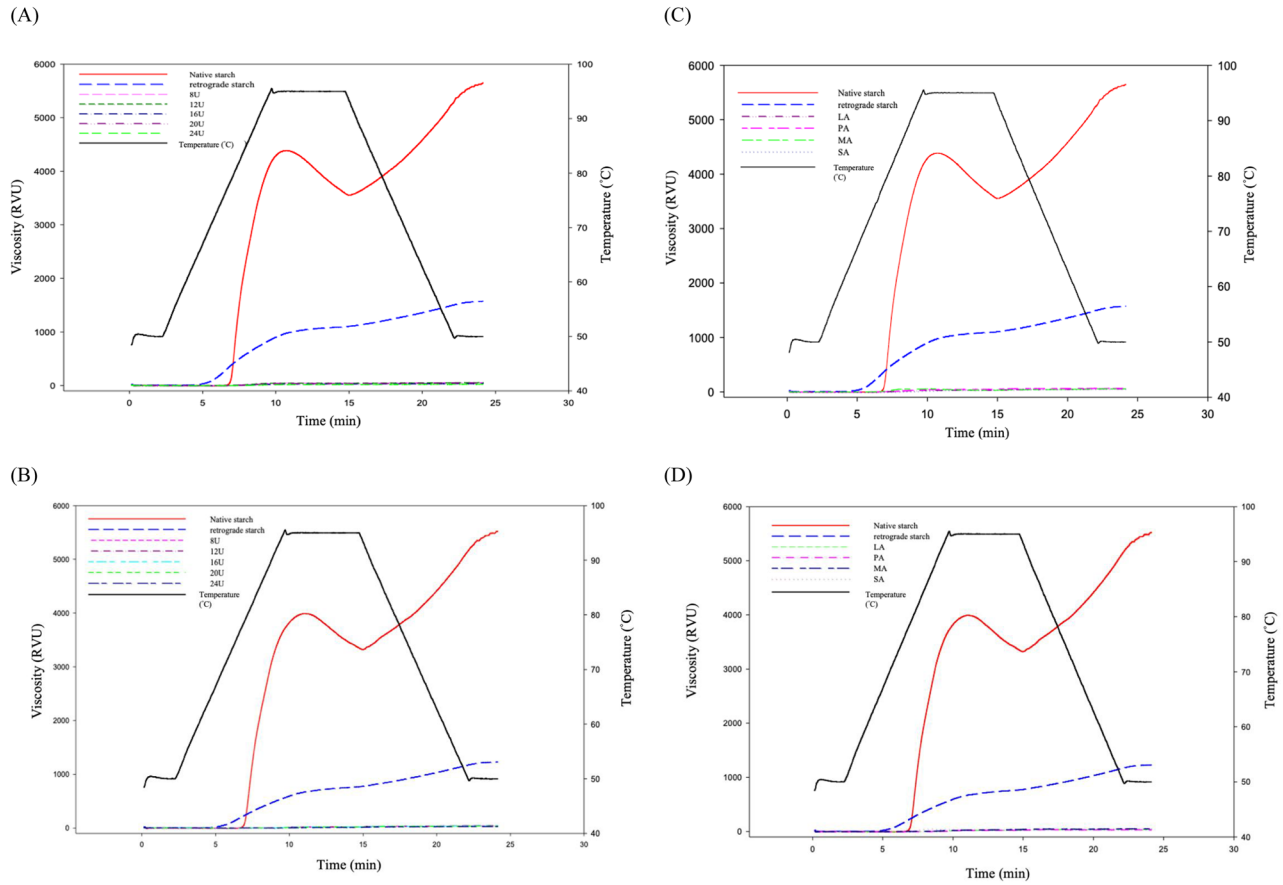

Fig. 2 | Viscoamylograms. A TNG1 treated with PD synergized FT, **B** TNG2 treated with PD synergized FT, **C** TNG1 treated with PD synergized FT and fatty acids addition, and **D** TNG2 treated with PD synergized FT and fatty acids addition.

collapsed, and irregularly shaped structures, while these results showed similarities to those of this study. Specifically, the starch particles appeared to be larger and more tightly packed, with the degree of alteration corresponding to the duration of the PD treatment.

In addition, this study showed an interesting characteristic of starch granules, which have a smooth network structure that partly covers them. Furthermore, the report from Tu et al.[31] supported the results of this study, which suggested that attachment occurs because these substances are a complex formed by lipid molecules with an amylose single helix, either on the surface or in the cavity of the starch granules. The quantity of these substances increases with FT cycle frequency and PD treatment effectiveness, producing more of these substances and causing them to adhere to the surface of the starch granules[31]. Moreover, it has been suggested that these structures are formed by the retrogradation process of starch, which increases the density of the crystal structure (ordered and stabilized state) and imparts hydrolysis-resistant properties to starch[52,77].

X-ray diffraction pattern (XRD)

Orderly arranged helices form the crystalline structure of starch, and crystallinity has been suggested to negatively correlate with digestibility[64,78]. However, the particle size and morphology of starches have been found to affect their bulk density and crystallinity, influencing their physicochemical and functional properties[79].

This study showed that native and retrograded yam starches (TNG1 and 2) exhibited absorption peaks at 5.58°, 14.4°, 17.2°, 22.2° and 24° at 2θ (Fig. 4A and B), which corresponded to the crystalline morphology of the rhizome starches, known as B-type[37,64,76]. However, both PD synergized FT-treated yam starches (TNG1 and 2) in this study showed intense absorption peaks at 5.5°, 17.2°, and 22.2°, whereas the absorption peaks at 15.10°, 17.2°, and 23.4° were weaker. It has been suggested that the change in the crystalline form of yam starch is related to the change of the crystalline form into the C-type[76].

Moreover, weak peaks were observed at 20.1° (Fig. 4C and D) with the addition of the four different fatty acids. It can be concluded that the starches were transformed into a C + V-type crystalline state[31,80]. Furthermore, PD treatment can effectively transform non-waxy rice starch from an A- to a B + V-type mixture[81]. V-type structures, reduced viscosity, improved solubility, and water-holding capacity have been reported in PD-modified maize, wheat, and pea starches[37]. Specifically, the V-type structure (containing six glucose units per turn (V6)) refers to amylase formation of left-handed single helices following the complexation of starch with guest compounds, with a central cavity to accommodate guests[50,82,83]. During this process, the crystalline properties of starch undergo a transformation that forms a V-type crystalline structure; namely, the hydrolysis of pullulanase leads to a more amorphous crystal structure[15,37]. This transformation mechanisms has been attributed to the formation of an inclusion complex between amylose and lipids (Fig. 5). Moreover, it is formed during food processing through interactions with non-covalent bonding (including hydrogen bonding, hydrophobic, and van der Waals forces)[84,85].

Regarding RC, the variance among the different types of starches can be attributed to various factors. These include the size of the starch crystal, number of crystalline regions, which is influenced by attributes such as amylopectin content and amylopectin chain length, the orientation of the double helices within the crystalline domains, and the degree of interaction between double helices[46]. As stated by Sherin et al.[86], the increased frequency of FT cycles during starch modification by FT treatment leads to the degradation of the amylopectin chains of the starch paste into shorter chain molecules. Consequently, this led to an increase in the water-holding capacity of the starch paste. In addition, digestive enzymes have fewer enzyme reaction sites for these short

Table 3 | Effects of paste properties via Pullulanase debranching (PD; 40 h), synergized freeze-thaw (FT) treatment, and four fatty acids' addition on the two yam varieties starches

Yam varieties	Status		Peak viscosity RVU	Holding strength	Breakdown	Final viscosity	Setback	Pasting temperature °C
Tainung No.1 (TNG1)	Native starch		4385.29 ± 65.15^{a}	3559.96 ± 73.25^{a}	826.65 ± 24.12^{a}	5649.75 ± 113.28^{a}	2090.58 ± 34.58^{b}	77.67 ± 2.35^{e}
	Retrograde starch[1]		1188.39 ± 15.78^{c}	902.59 ± 29.38^{c}	286.69 ± 17.16^{c}	1574.59 ± 79.63^{c}	672.66 ± 17.28^{c}	64.62 ± 2.41^{g}
	Pullulanase debranching (PD) synergized freeze-thaw (FT) 1-cycle	8U[2]	46.21 ± 2.35^{e}	31.15 ± 1.17^{e}	15.23 ± 0.46^{h}	57.25 ± 2.59^{f}	26.36 ± 1.92^{h}	73.95 ± 1.35^{f}
		12U	44.15 ± 2.02^{f}	28.23 ± 1.12^{f}	16.63 ± 0.55^{gh}	63.36 ± 3.24^{e}	35.73 ± 1.09^{e}	74.42 ± 1.17^{f}
		16U	30.96 ± 1.02^{j}	13.01 ± 0.26^{h}	17.36 ± 0.24^{g}	37.39 ± 1.48^{j}	24.09 ± 1.15^{i}	80.35 ± 2.03^{d}
		20U	36.33 ± 1.12^{g}	21.15 ± 0.06^{g}	16.69 ± 0.36^{gh}	50.29 ± 2.56^{g}	29.03 ± 1.09^{g}	77.92 ± 1.95^{e}
		24U	18.37 ± 1.52^{l}	1.07 ± 0.07^{j}	17.62 ± 0.25^{g}	25.17 ± 1.71^{l}	24.07 ± 1.51^{i}	92.12 ± 1.25^{a}
	Lipid	LA[3]	43.46 ± 2.19^{h}	27.16 ± 2.25^{g}	16.16 ± 0.52^{h}	55.29 ± 3.48^{h}	28.36 ± 1.82^{g}	76.77 ± 1.17^{e}
		PA	57.69 ± 3.42^{e}	29.13 ± 0.46^{f}	28.14 ± 0.36^{e}	57.58 ± 3.28^{fg}	28.33 ± 1.52^{g}	71.51 ± 1.41^{f}
		MA	58.18 ± 2.57^{e}	40.33 ± 2.58^{e}	18.36 ± 0.29^{g}	66.97 ± 3.25^{e}	26.31 ± 1.08^{h}	76.43 ± 1.25^{e}
		SA	49.22 ± 2.35^{f}	22.31 ± 1.25^{h}	27.33 ± 0.36^{e}	56.13 ± 1.25^{gh}	34.12 ± 1.79^{e}	81.16 ± 1.52^{d}
Tainung No.2 (TNG2)	Native starch		3987.65 ± 71.52^{b}	3328.95 ± 78.47^{b}	659.84 ± 81.26^{b}	5523.79 ± 73.21^{b}	2195.63 ± 74.52^{a}	79.54 ± 1.43^{d}
	Retrograde starch		864.36 ± 13.25^{d}	596.96 ± 31.25^{d}	268.15 ± 36.46^{d}	1229.35 ± 29.24^{d}	633.39 ± 26.33^{d}	66.27 ± 1.26^{g}
	PD synergized FT 1-cycle	8	33.12 ± 0.52^{hi}	1.07 ± 0.03^{h}	20.23 ± 0.86^{f}	41.36 ± 1.25^{i}	28.31 ± 0.96^{g}	81.57 ± 2.06^{d}
		12	34.15 ± 0.36^{h}	12.16 ± 0.23^{hi}	22.19 ± 0.75^{e}	43.33 ± 1.29^{h}	31.16 ± 1.23^{f}	86.85 ± 1.15^{c}
		16	32.36 ± 0.19^{l}	12.26 ± 1.07^{hi}	20.33 ± 0.77^{f}	41.15 ± 1.09^{j}	29.36 ± 1.15^{g}	87.67 ± 1.75^{bc}
		20	33.56 ± 1.07^{hi}	11.06 ± 0.76^{i}	22.16 ± 0.46^{ef}	40.19 ± 1.28^{i}	29.19 ± 1.07^{g}	87.66 ± 1.78^{bc}
		24	23.19 ± 0.34^{k}	2.02 ± 0.06^{j}	21.15 ± 0.62^{ef}	30.25 ± 1.47^{k}	28.32 ± 1.17^{g}	95.34 ± 1.29^{a}
	Lipid	LA	36.36 ± 1.82^{i}	16.23 ± 0.36^{j}	20.19 ± 0.37^{f}	39.53 ± 1.68^{j}	23.33 ± 1.07^{i}	88.37 ± 1.17^{b}
		PA	46.36 ± 0.59^{g}	18.39 ± 1.15^{i}	28.18 ± 0.23^{e}	49.28 ± 1.45^{i}	31.19 ± 1.22^{f}	81.15 ± 1.52^{d}
		MA	34.63 ± 1.25^{j}	13.03 ± 0.64^{k}	21.16 ± 1.26^{f}	33.23 ± 1.41^{k}	20.33 ± 1.07^{j}	90.19 ± 1.36^{b}
		SA	47.17 ± 0.88^{g}	30.13 ± 0.26^{f}	17.13 ± 1.06^{gh}	58.69 ± 1.75^{f}	28.19 ± 1.15^{g}	72.77 ± 1.52^{f}

[1] Retrograde starch: freeze-thawing 1 cycle for 24 h.
[2] Pullulanase activity (U/g starch).
[3] Lauric acid (LA; C12); Myristic acid (MA; C14), Palmitic acid (PA; C16), and Stearic acid (SA; C18).
Different lowercase letters labeled in the same row represent significant differences ($p < 0.05$).

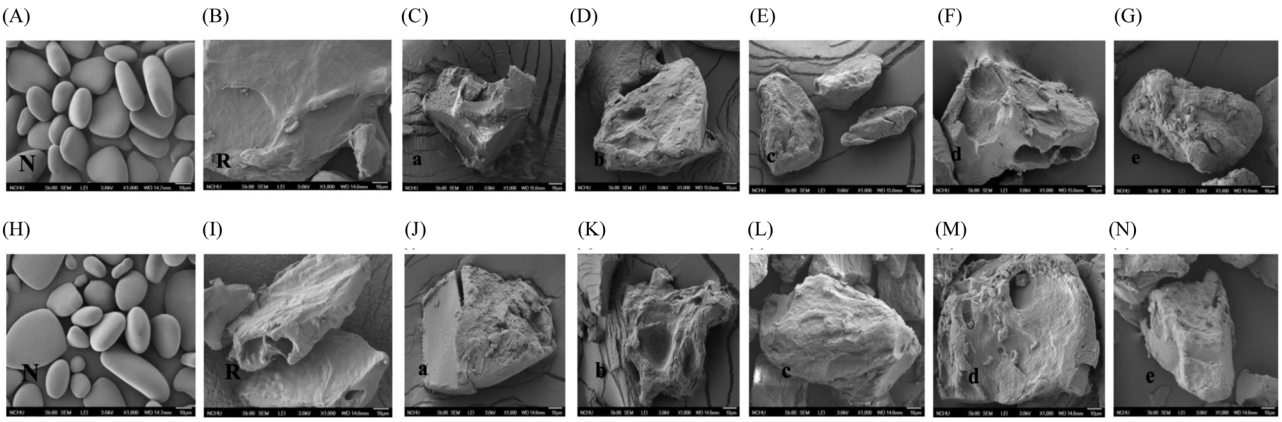

Fig. 3 | Microstructures of yam starches. TNG1: A native starch; B retrograded starch; C–G: PD (8, 12, 16, 20 and 24 U) synergized FT and TNG2: H native starch; I retrograded starch; H–N: PD (8, 12, 16, 20 and 24 U) synergized FT.

chains than for long chains; namely, a negative correlation between the percentage of starch hydrolysis and the ratio of short- and long-branched chains has been reported[80,87]. During freezing, the water combines with the degraded amylopectin, expelling water that would otherwise have been absorbed[88]. According to Li et al.[88], accelerated starch retrogradation is beneficial for producing pasta, particularly vermicelli. This observation implies that starch retrogradation can be used to improve the quality and texture of pasta products through improved formulation and process optimization.

This study showed that native yam starches TNG1 and 2 were 42.17 and 32.53%, respectively (Table 4), whereas a tendency to increase and decrease RC occurred for PD combined with FT treatments. However, it has been reported that the increased duration of PD treatment of starch synergistically with sterilization results in a higher RS content and consequently contributes to the increase in RC[12]. Nonetheless, this study failed to reveal any evidence of dose dependence in PD treatment. In particular, TNG1 (8U) and 2 (8 and 24U) demonstrated a significant increase in RC, which was not included in the trend, as mentioned earlier, or published.

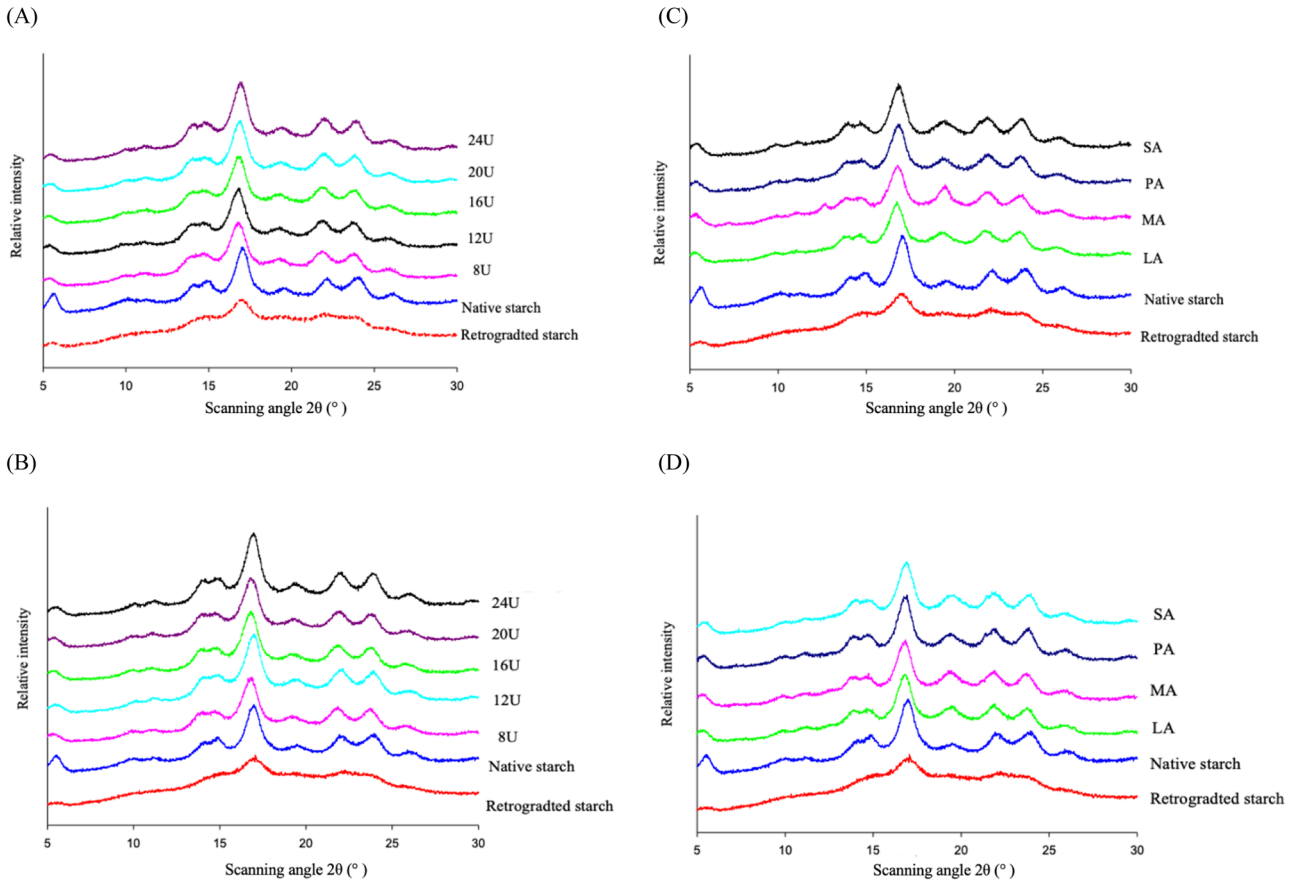

Fig. 4 | Crystalline structures of yam starches. A TNG1 treated with PD synergized FT; **B** TNG2 treated with PD synergized FT ; **C** TNG1 treated with PD synergized FT and fatty acids addition and **D** TNG2 treated with PD synergized FT and fatty acids addition.

This study postulated that potential discrepancies could arise from the different sources of starch, despite all belonging to B-type rhizomes, which may affect the outcome of the study. Therefore, it is imperative to consider these factors when conducting more profound analyses and interpreting the results. Another possible reason might be that FT treatment disrupted and rearranged the amorphous region; thus, the RC of starch increased[32,89]. Moreover, the RC of TNG1 showed a significant increase in the presence of PA and SA, whereas the RC of TNG2 showed a slight increase in the groups supplemented with LA and PA. Therefore, TNG1 treatment with pullulanase (8U) provided a similar RC-enhancing effect as the addition of PA or SA, whereas TNG2 using pullulanase (8 and 24U), LA, or PA provided a similar RC-enhancing effect.

Estimate GI (eGI)

GI is a well-established metric that determines the extent to which food containing carbohydrates can trigger an increase in blood sugar levels[41,78,90]. The reference food for GI is white bread or glucose, with a GI value of 100. Foods with GI values equal to or greater than 70 are classified as high-GI foods, those with GI values between 56 and 69 are medium GI foods, and those with GI foods ≥ 55 are classified as low GI foods[78,82]. Furthermore, HI, a derivative linked to starch digestibility, has been utilized to approximate GI[82,91].

This study showed that the GI of yam starches (TNG1 and 2) treated with PD combined with FT tended to decrease compared to that of gelatinized and retrograded starches (Table 4). The GIs of 20U + FT of TNG1 (73.856) and 8U + FT of TNG2 (69.648) exhibited the most significant decreases. This also means that the GI values of the PD synergized FT-modified yam starches did not improve, despite previous results showing a satisfactory digestibility with RS and C + V-type crystalline states. In other words, yam starches with different treatment conditions would become high- or medium-GI foods, which could induce postprandial glycemic spikes. To clarify, yam starches undergoing varying treatment conditions will likely turn into high- or moderate-GI foods, causing postprandial glycemic spikes[82]. This situation has burdened the mechanisms regulating post-meal blood glucose levels that are essential for health, particularly metabolic diseases (cardiovascular diseases, obesity, type 2 diabetes, and colon cancer)[16,78,92]. This issue requires prompt attention to avoid health risks. However, no dose-dependent effects were observed in this study. While PD treatment followed by the addition of adding diverse fatty acids produced parallel results, TNG1 with MA exhibited the most notable decrease in GI (Table 4). In contrast, TNG2 showed a declining GI trend for all four fatty acids (LA, PA, MA, and SA). These phenomena may be attributed to the PD treatment, which increased amylose content and decreased RDS and SDS content, followed by FT treatment, where retrogradation of starch led to an increase in RS content, thereby affecting the GI of yam starch. It is worth noting that these results were also echoed in the above study. However, several studies have demonstrated that in vitro estimates and in vivo analyses are consistent with each other[82,93]. These findings support the notion that in vitro assays can be reliable surrogates for predicting in vivo outcomes. The process is challenging and requires further technological innovations to elevate the current in vitro and in vivo models to a higher level that is more relevant to the actual[94]. Moreover, the results of this study demonstrate that combining TNG2 yam starch with PD, FT treatment, and LA, MA, or SA produces a definition consistent with low GI foods. However, other treatments did not have a significant modifying effect. This finding suggests that a combination of TNG2 yam starch and treatments can be used as an ingredient in low-GI food products. Further investigation is guaranteed to determine the factors contributing to these observations.

In conclusion, the results of this study demonstrate that the inclusion of fatty acids and gelatinization of yam (TNG1 and 2) starches through PD

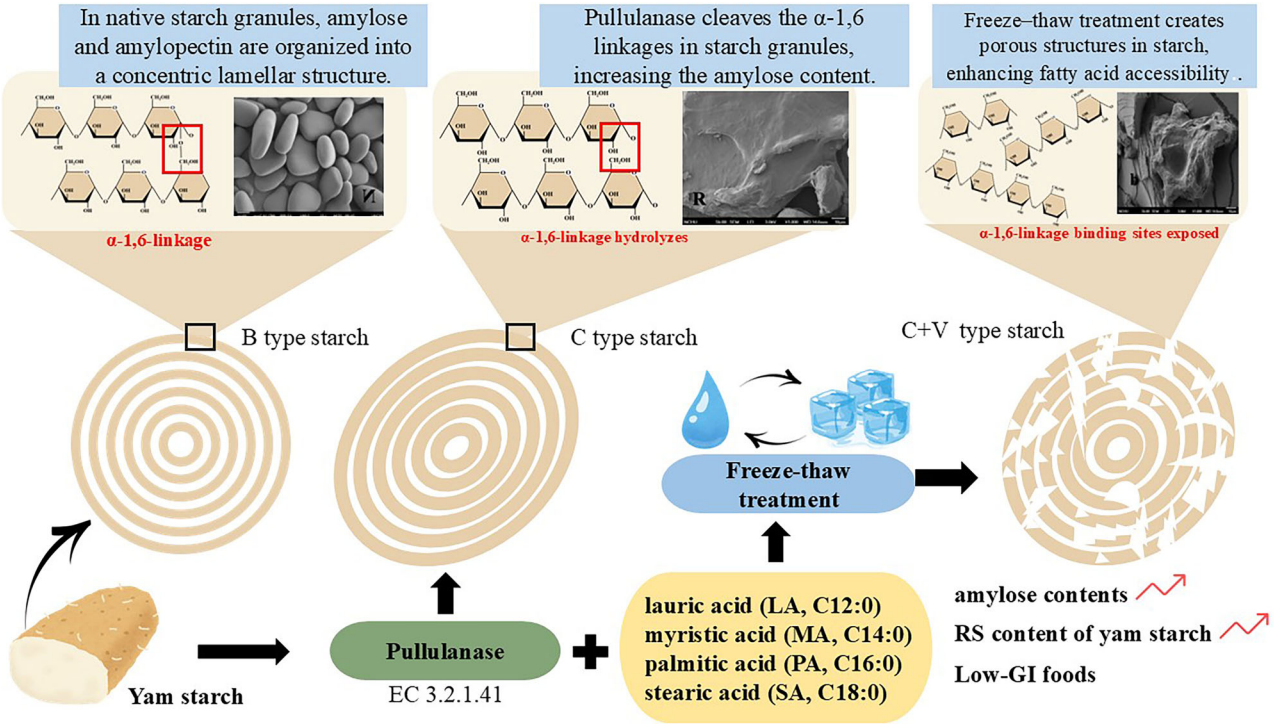

Fig. 5 | Mechanism diagrams of yam starches treated with PD, fatty acids and synergized FT.

(20U for 40 h) synergized with FT (1 cycle) treatment can significantly increase the RS content and RC. Furthermore, these processes were observed to cause a shift in the crystalline morphology of the starches from B- to C- and C + V-types. These findings suggest that the gelatinization of yam starch may have potential applications in the development of functional foods and supplements and warrants further investigation. The practical effect of modified yam starch in reducing GI demands future in vivo validation, such as through further gastrointestinal digestion modeling or clinical trials. Moreover, this study provides an all-inclusive understanding of yam starch, which can be used as a reference point in future research concerning developing low-GI food products. The collection of essential information, such as yam starch, was meticulously and systematically examined, providing a reliable and comprehensive source of information for researchers and professionals.

Methods

Materials

Different kinds of yam starches were used in this study, extracted from two types of yams, TNG1 and 2 yams (*Dioscorea alata* L.); harvested nine months post-planting (March–December 2023). The yams were procured from Ming-Jian Township No.1 Production and Marketing Workshop farmers (Nantou, Taiwan) and subsequently extracted within our laboratory (described in the next section). All chemicals used in this study, including fatty acids, such as LA (C12), MA (C14), PA (C16), and SA (C18), were purchased from Sigma-Aldrich® (Merck KGaA, Darmstadt, Germany). Pullulanase (EC 3.2.1.41, Promozyme® D6, 1,496 New Pullulanase Unit Novo (NPUN)/mL) was purchased from Novozymes A/S (Bagsværd, Denmark).

Extraction of yam starches

The yam was washed, peeled, cut into cubes, weighed 2 kg, then homogenized with a sodium bisulfite solution (0.075%) in a blender, sieved with a 200-mesh sieve, and the filtrate collected. The residue was collected as described above. All filtrates were mixed and stored at 4 °C overnight; the resulting slurry is then filtered and sieved to separate the starch from other impurities. The residue was mixed with a 5-fold volume of 0.1% NaOH (*w/v*) and collected by centrifugation (6000 × *g*). The above procedure was repeated using distilled water until the pH reached 7.0. Next, the yam starch was washed with 5-fold volumes of 70% ethanol (*v/v*), dried at 40 °C, ground, and sieved (100 mesh) to obtain the yam starch. All starches were packed in double zip-lock bags and kept at −20 °C for freezing until further use.

PD synergized FT treatments of starches

This modification was carried out following the methods depicted by Miao et al.[46] and Pongjanta et al.[52]. Starch was prepared as a 10% starch suspension (200 mL) and placed in a water bath at 30 °C for 1 h with intermittent shaking (170 rpm). Then, the starch solution was heated at 100 °C for 30 min. Next, at 55 °C, pullulanase enzymes (8, 12, 16, 20, and 24 NPUN/g starch) were added for the starch debranching treatment. The starch was then immersed in a water bath at 55 °C with shaking (170 rpm) for 40 h. In addition, the partially above PD-treated samples (debranched starch solutions) were mixed with four fatty acids: LA, MA, PA, and SA (2% dry starch base, dry weight basis; *w/w*). Subsequently, all samples were heated at 100 °C for 30 min (to stop the enzymatic reaction and uniformly mix the fatty acids with the starch paste) and then cooled to 25 °C.

All the above samples were subjected to FT 1 cycle processing, stored at −20 °C for 24 h, and thawed at 30 °C for 24 h. The samples were then dried in hot air at 45 °C, for 12 h. Afterwards, the starch granules were manually reduced to smaller particles with the aid of a mortar and standardized on a 0.250 mm sieve supernatant. Similarly, all samples were packed in double zip-lock bags and frozen until further use.

Determination of amylose content

The method described by Gunaratne and Hoover[57] was used to determine the amylose content of the starches. The starch sample (20 mg) was added to 8 mL of 90% dimethyl sulfoxide (DMSO) and subsequently immersed in a water bath at 85 °C and shaken for 15 min. The mixture was then cooled to 25 °C. Subsequently, it was diluted to 25 mL with distilled water. Next, 10 mL of the above mixture was added to 5 mL of iodine solution (0.0025 M I_2 and 0.0065 M KI), mixed evenly, then the volume was quantified to 50 mL with distilled water. Finally, it was allowed to stand for 15 minutes until the

Table 4 | Effects of relative crystallinity, the crystalline type, hydrolysis index (HI), and estimated glycemic index (eGI) via Pullulanase debranching (PD; 40 h) synergized freeze-thaw (FT) treatment, and four fatty acids' addition on the two yam varieties' starches

Yam varieties	Status		Relative crystallinity (%)	X-ray pattern	Hydrolysis Index (HI)	Glycemic Index (GI)
Tainung No.1 (TNG1)	Native starch		42.17 ± 0.53^{c}	B	-[5]	
	Gelatinized starch[1]		-		89.66 ± 1.42^{a}	88.44 ± 3.02^{a}
	Retrograde starch[2]		31.38 ± 0.78^{f}	B	72.71 ± 2.03^{c}	79.13 ± 2.58^{b}
	Pullulanase debranching (PD) synergized freeze-thaw (FT) 1-cycle	8U[3]	45.02 ± 0.63^{b}	C	60.91 ± 1.55^{e}	72.65 ± 2.14^{d}
		12U	40.91 ± 0.69^{c}	C	77.43 ± 1.37^{b}	81.72 ± 2.15^{b}
		16U	40.99 ± 0.71^{c}	C	71.31 ± 2.02^{c}	78.36 ± 1.53^{b}
		20U	36.02 ± 0.52^{d}	C	63.11 ± 1.39^{e}	73.86 ± 1.28^{d}
		24U	37.01 ± 0.45^{d}	C	67.95 ± 1.15^{d}	76.52 ± 1.08^{c}
	Lipid	LA[4]	40.12 ± 0.39^{c}	C + V	75.74 ± 2.24^{b}	80.80 ± 1.63^{b}
		PA	38.37 ± 0.38^{d}	C + V	69.16 ± 1.36^{d}	77.20 ± 1.15^{b}
		MA	44.89 ± 0.32^{b}	C + V	53.47 ± 1.54^{f}	68.56 ± 2.21^{e}
		SA	49.68 ± 0.34^{a}	C + V	76.10 ± 2.05^{b}	80.98 ± 1.26^{b}
Tainung No.2 (TNG2)	Native starch		32.53 ± 0.35^{e}	B	-	
	Gelatinized starch		-		91.35 ± 1.95^{a}	89.36 ± 1.74^{a}
	Retrograde starch		32.00 ± 0.25^{e}	B	76.86 ± 1.63^{b}	81.41 ± 1.52^{b}
	PD synergized FT 1-cycle	8	45.42 ± 0.36^{b}	C	69.65 ± 1.26^{d}	77.45 ± 1.29^{b}
		12	30.85 ± 0.38^{f}	C	74.90 ± 1.37^{b}	80.33 ± 1.48^{b}
		16	33.25 ± 0.42^{e}	C	78.41 ± 1.52^{b}	82.26 ± 1.33^{b}
		20	31.25 ± 0.51^{e}	C	73.91 ± 1.15^{b}	79.79 ± 2.08^{b}
		24	51.92 ± 0.45^{a}	C	76.30 ± 1.29^{b}	81.10 ± 1.26^{b}
	Lipid	LA	45.51 ± 0.41^{b}	C + V	38.24 ± 1.18^{g}	60.20 ± 1.53^{f}
		PA	39.25 ± 0.24^{c}	C + V	57.02 ± 2.02^{e}	70.51 ± 1.87^{d}
		MA	44.03 ± 0.33^{b}	C + V	31.72 ± 2.14^{g}	56.62 ± 1.26^{f}
		SA	39.95 ± 0.36^{c}	C + V	35.16 ± 1.55^{g}	58.51 ± 1.51^{f}

[1] Gelatinize starch: native starch heat at boiling water (100 °C) for 1 h.
[2] Retrograde starch: freeze-thawing 1 cycle for 24 h.
[3] Pullulanase activity (U/g starch).
[4] Lauric acid (LA; C12); Myristic acid (MA; C14), Palmitic acid (PA; C16), and Stearic acid (SA; C18).
[5] Not measured.
Different lowercase letters labeled in the same column represent significant differences ($p < 0.05$).

color changed. At the same time, the absorbance value was determined by a spectrophotometer (Model U-2001 Hitachi Co., Tokyo, Japan) at a wavelength of 600 nm. The amylose content of the samples was calculated by interpolation against a standard curve prepared from pure amylose from potatoes.

Determination of MW distributions

The MW distributions of the samples in this study were determined based on the method described by Liu et al.[37] with some modifications. A standard curve was prepared using Pullulan standards (Shodex P-82, Resonac Holdings Co., Ltd., Tokyo, Japan). Analyses were performed using gel permeation chromatography (GPC). Subsequently, 15 mL of 90% DMSO was added to 75 mg of the sample to create a starch suspension. The mixture was then heated for 1 h at 100 °C and stirred for 24 h at 25 °C. The supernatant was then mixed with a 4-fold volume of 95% ethanol (*v*/*v*) and left to stand for 10 min, followed by centrifugation at 6000× *g* for 10 min before eliminating the supernatant. The residue was mixed with 15 mL hot distilled water at 100 °C and placed in a water bath at 100 °C for 1 h. Finally, it was filtered through a 5 μm polyvinylidene fluoride (PVDF) membrane and reserved for use. Subsequently, 5 mL of the filtrate sample was loaded into a Sephacryl™ S-400HR 16/60 column (GE Healthcare, Chicago, IL, USA) and stored at 40 °C for further analysis. The samples were detected using a refractive index detector (RI-8020, Tosoh Co., Tokyo, Japan). In addition, the column was equilibrated with a mobile phase of 0.2% NaCl/0.05 M NaOH for elution before application. A standard curve was prepared using Pullulan standards (Shodex P-82, Resonac Holdings Co., Ltd., Tokyo, Japan). The interpolation method was employed to calculate the MW distribution in the sample.

In vitro digestibility

The starch digestibility was determined using the Megazyme® Digestible and RS Assay Kit (Megazyme Ltd., Bray, Ireland). The analysis was performed following the standard operating procedures (SOP) provided by the manufacturer. Contents of rapidly digested starch (RDS, digested for 20–120 min) and SDS (digested for 20 min). Briefly, the sample (100 mg) was mixed with 4 mL of α-amylase (10 mg/mL containing 3 U/mL amyloglucosidase (AMG)) and immersed for 20 and 120 min at 37 °C in a water bath with shaking (200 rpm). Then, 4 mL of 99% ethanol was added, and the supernatant was collected by centrifugation (6000× *g*, 10 min). The residue was added to 4 mL of 50% ethanol, centrifuged (6000× *g*, 10 min), and repeated twice. All collected supernatants were quantified to 100 mL with 0.1 M sodium acetate buffer (pH 4.5). Subsequently, 0.1 mL of the previously mentioned mixture was introduced to 3 mL of glucose oxidase peroxidase (GOPOD) solvent, and the resulting mixture was subjected to a reaction in a water bath at 50 °C for 20 min. The absorbance of the final solution was measured at 510 nm. The RDS and SDS values of the samples

were calculated using the following formula:

$$\text{Rapidly digestible starch(RDS;\%)} = (G20 - G0) \times 0.9 \quad (1)$$

$$\text{Slowly digestible starch(SDS;\%)} = (G120 - G20) \times 0.9 \quad (2)$$

where, G0, G20, and G120 represent the glucose percentage in the enzymatic hydrolysis at 0, 20, and 120 min, respectively.

Determination of RS content and eGI

The RS content of the sample was analyzed using Megazyme® resist starch kits (Megazyme Ltd., Bray, Ireland), following the SOP provided by the manufacturer's protocol. The procedure involved weighing the samples (100 mg) in centrifuge tubes. Subsequently, 4 mL of pancreatic α-amylase (10 mg/mL containing 3 U/mL AMG) was added to the tubes to ensure thorough and even mixing. The mixture was immersed for 16 h at 37 °C in a water bath. Next, 4 mL of 99% ethanol was added, the tubes were centrifuged (6000× *g* for 10 min) using a highly efficient centrifuge (CR22F, Hitachi Co.), and the supernatant was collected. The residue was mixed with 4 mL of 50% ethanol, centrifuged (6000× *g* for 10 min), and repeated twice. Subsequently, all supernatants were quantified to 100 mL with 0.1 M sodium acetate buffer solution (pH 4.5). Subsequently, 2 mL of 2 M KOH was added and mixed evenly. The solution was then stirred for 20 min in an ice bath. Then, 8 mL of 1.2 M acetic acid buffer solution (pH 3.8) and 0.1 mL of AMG (3300 U/mL) were added. The solution was then immersed for 30 min in a 50 °C water bath before centrifugation (6000× *g* for 10 min). The supernatant (0.1 mL) was mixed with 3 mL of GOPOD reagent and immersed at 50 °C for 20 min in a water bath. The absorbance was measured at 510 nm. The standard was established using 100 μg of glucose, and the steps mentioned above were repeated. The RS contents of the samples were determined using the following formula:

$$\begin{aligned} \textit{Resistant starch}\ (\tfrac{g}{100g}\ \textit{sample}) = {} & \textit{Absorbance}\ 510\ \textit{nm of the sample} \\ & \times \textit{Absorbance}\ 510\ \textit{nm of}\ 100\ \mu g\ \textit{glucose}/\textit{Sample weight} \times 90 \end{aligned} \quad (3)$$

The eGI of the sample was determined and calculated using the method described by Li et al.[91], with slight modifications. A solution containing 10% starch was sterilized in an autoclave at a temperature of 105 °C for 10 min. Next, the sample was added with 0.2 mL pepsin and 5 mL α-amylase (2.6 U) at 37 °C in a water bath with shaking at 200 rpm for 30–180 min. Every 30 min, 1 mL was dispensed, and the sample was heated at 100 °C for 5 min to inactivate the enzyme. Then, 3 mL of acetic acid buffer solution (0.4 M, pH 4.75) was added, accompanied by 60 μL of AMG. The mixture was agitated for 45 min at 60 °C to induce the digestion of starch into glucose. The samples were subjected to serial dilution with deionized water in the 10–100 mL range, followed by 0.5 mL of each sample combined with 3 mL of GOPOD reagent. The absorbance of each sample was measured at 510 nm to determine glucose content. The GI of the sample and the hydrolysis index (HI) were determined, and the sample was prepared by defining the hydrolysis area of 50 mg of glucose as 100. The following equation utilizes this HI value to calculate the GI of the sample:

$$\text{Estimate of the Glycemic Index(eGI)} = 39.71 + 0.549(\text{HI}) \quad (4)$$

Thermal properties

The thermal properties of starch were determined according to the method described by Lin et al.[95], with slight modifications. The starch sample (80 mg) was added to distilled water (240 mg), sealed, and hydrated for 1 h before analysis using a micro differential scanning calorimeter (μDSC; Setaram Model VII Micro DSC, KEP Technologies, Provence-Alpes-Côte d'Azur, France). The temperature increased from 25 to 120 °C at a controlled rate of 1.2 °C/min, followed by a decrease back to 25 °C at the same rate. The onset temperature (To), peak temperature (Tp), and end temperature (Tc) of the paste, along with the calculation of the paste enthalpy (Δ*H*; mJ/g) from the thermal absorption curve of the sample.

Paste properties

The viscosity of the paste was measured using the method described by Huang et al.[96]. The sample was prepared as an 8% starch suspension solution, and the paste properties were determined using a Rapid Visco Analyzer (RVA; Model RVA-3D, Newport Scientific, Sydney, Australia). Briefly, starch slurries were heated to 95 °C at 6 °C/min and held at that temperature for 5 min. Then, it was cooled to 50 °C at the same rate and held at that temperature for 2 min, for a total of 24 min for the entire trial. At the beginning of the trial, the slurries were equilibrated at 50 °C for 1 min. The pasting curves of RVA offer a comprehensive range of starch properties, including but not limited to peak viscosity (PV), final viscosity (FV), breakdown (BD), hot paste viscosity (HPV), setback (SB), peak time, and pasting temperature.

Granules morphology

The morphology of the sample granules was determined using the method described in Huang et al.[97], with some modifications. The 0.5 g starch sample was plated with platinum for two minutes under a vacuum degree of 2.4 Pa. A field emission scanning electron microscope (SEM; JSM-7100F, JEOL Ltd., Tokyo, Japan) at an accelerating voltage of 3 kV was used. The SEM observed the starch's particle size and surface structure at 1,000-fold magnification.

X-ray diffraction pattern (XRD)

The crystalline structure and crystallinity of the starch samples were determined according to the method described by Cheng et al.[98], with slight modifications. The procedure involved placing a sample weighing 1.0 g on a microscope slide (25×35×1 mm). Subsequently, the sample was equilibrated for 14 days in a closed desiccator filled with a saturated silver chloride solution. A starch sample weighing 1 g was analyzed by X-ray diffraction (XRD; Model D5000, Siemens Co., München, Germany). The analytical conditions were set at 40 kV and 30 mA operating current, and the scanning speed 0.02°/s. The scanning angle 2θ was varied from 4° to 30° to obtain the necessary data. To generate an XDR spectrum, the degree of crystallinity of starch was assessed using the Find Graph software (V2.622, UNIPHIZ Lab, Greensburg, PA, USA). The crystallinity value of starch was calculated as the area between the smooth curve and the baseline, while the area between the curve and the peak indicated the RC under the peak.

$$\begin{aligned} \textit{Relativecrystallinity}\ (\%; \text{RC}) = {} & \textit{Crystalline area}/(\textit{Crystalline area} \\ & + \textit{Amorphous area}) \times 100 \end{aligned} \quad (5)$$

Statistical analysis

All the trials in this study had at least three replicates ($n \geq 3$). This study's results are presented as the average value of the data, known as the mean ± standard deviation (SD). All data were analyzed for variability within samples using one-way ANOVA, and Duncan's multiple range tests with SAS software (V9.4, SAS Institute, Cary, NC, USA) were used to determine the significance of the differences between groups. A *p*-value of less than 0.05 was considered statistically significant.

Data availability

Data available within the article or its supplementary materials.

Code availability

Not applicable.

Received: 30 December 2024; Accepted: 4 October 2025;
Published online: 11 December 2025

References

1. Ochoa, S. & Osorio-Tobón, J. F. Isolation and characterization of starch from the purple yam (Dioscorea alata) anthocyanin extraction residue obtained by ultrasound-assisted extraction. *Waste Biomass-. Valoriz.* **15**, 379–389, https://doi.org/10.1007/s12649-023-02155-y (2024).
2. Hou, W. C., Hsu, F. L. & Lee, M. H. Yam (Dioscorea batatas) tuber mucilage exhibited antioxidant activities in vitro. *Planta Med.* **68**, 1072–1076, https://doi.org/10.1055/s-2002-36356 (2002).
3. Zou, J. et al. Structure and processing properties of nine yam (Dioscorea opposita Thunb) starches from South China: a comparison study. *Molecules* **27**, 2254, https://doi.org/10.3390/molecules27072254 (2022).
4. Xiao, Y. et al. Cultivation pattern affects starch structure and physicochemical properties of yam (Dioscorea persimilis). *Int. J. Biol. Macromol.* **242**, 125004. https://doi.org/10.1016/j.ijbiomac.2023.125004 (2023).
5. Otegbayo, B. O., Tanimola, A. R., Ricci, J. & Gibert, O. Thermal properties and dynamic rheological characterization of dioscorea starch gels. *Gels* **10**, 51, https://doi.org/10.3390/gels10010051 (2024).
6. Faluyi, J. O., Matthew, J. O. & Azeez, S. O. Collection, characterizaton, product quality evaluation, and conservation of genetic resources of yam (Dioscorea spp.) cultivars from Ekiti State, Nigeria. *Genet. Resour. Crop Evol.* **69**, 1419–1437, https://doi.org/10.1007/s10722-022-01349-y (2022).
7. Asiamah, E. et al. Effect of xanthan gum and carboxymethyl cellulose on structure, functional and sensorial properties of yam balls. *Heliyon* **8**, e11200. https://doi.org/10.1016/j.heliyon.2022.e11200 (2022).
8. Nwosu-Obieogu, K. et al. Three leaved yam starch physical / engineering properties evaluation using Response Surface Methodology and Artificial Neural Network network. *J. Agric. Food Res.* **14**, 100746. https://doi.org/10.1016/j.jafr.2023.100746 (2023).
9. Li, L., Chen, J., Zhou, S., Ren, G. & Duan, X. Quality evaluation of probiotics enriched Chinese yam snacks produced using infrared-assisted spouted bed drying. *J. Food Process. Preserv.* **45**, e15358. https://doi.org/10.1111/jfpp.15358 (2021).
10. Shi, M. et al. Effect of extrusion on the formation, structure and properties of yam starch-gallic acid complexes. *Int. J. Biol. Macromol.* **264**, 130461. https://doi.org/10.1016/j.ijbiomac.2024.130461 (2024).
11. Jiang, S. et al. Physicochemical characterizations of five Dioscorea alata L. starches from China. *Int. J. Biol. Macromol.* **237**, 124225. https://doi.org/10.1016/j.ijbiomac.2023.124225 (2023).
12. Bodjrenou, D. M. et al. Effect of pullulanase debranching time combined with autoclaving on the structural, physicochemical properties, and in vitro digestibility of purple sweet potato starch. *Foods* **11**, 3779, https://doi.org/10.3390/foods11233779 (2022).
13. Verma, D. K. & Srivastav, P. P. Isolation, modification, and characterization of rice starch with emphasis on functional properties and industrial application: a review. *Crit. Rev. Food Sci. Nutr.* **62**, 6577–6604, https://doi.org/10.1080/10408398.2021.1903383 (2022).
14. Chakraborty, I., Pallen, S., Shetty, Y., Roy, N. & Mazumder, N. Advanced microscopy techniques for revealing molecular structure of starch granules. *Biophys. Rev.* **12**, 105–122, https://doi.org/10.1007/s12551-020-00614-7 (2020).
15. Zheng, F. et al. Multi-scale structural characteristics of black Tartary buckwheat resistant starch by autoclaving combined with debranching modification. *Int. J. Biol. Macromol.* **249**, 126102. https://doi.org/10.1016/j.ijbiomac.2023.126102 (2023).
16. Liu, Z., Liu, L., Han, P. & Liang, X. Pea resistant starch preparation with cold-active type I pullulanase from Bacillus megaterium and its potential application in rice noodles. *LWT* **182**, 114799. https://doi.org/10.1016/j.lwt.2023.114799 (2023).
17. Das, M., Rajan, N., Biswas, P. & Banerjee, R. A novel approach for resistant starch production from green banana flour using amylopullulanase. *LWT* **153**, 112391. https://doi.org/10.1016/j.lwt.2021.112391 (2022).
18. Amaraweera, S. M. et al. Development of starch-based materials using current modification techniques and their applications: A review. *Molecules* **26**, 6880, https://doi.org/10.3390/molecules26226880 (2021).
19. Kumari, B. & Sit, N. Comprehensive review on single and dual modification of starch: Methods, properties and applications. *Int. J. Biol. Macromol.* **253**, 126952. https://doi.org/10.1016/j.ijbiomac.2023.126952 (2023).
20. Su, L. & Wu, J. In *Industrial Starch Debranching Enzymes* (eds J. Wu & W. Xia) 225–267 (Springer Nature Singapore, 2023).
21. Jin, Y. et al. Physicochemical characterization of debranched waxy rice starches and their effect on the quality of low-fat ice cream mixtures. *Food Biosci.* **57**, 103485. https://doi.org/10.1016/j.fbio.2023.103485 (2024).
22. Niu, D., Cong, H., Zhang, Y., McHunu, N. P. & Wang, Z.-X. Pullulanase with high temperature and low pH optima improved starch saccharification efficiency. *Sci. Rep.* **12**, 21942. https://doi.org/10.1038/s41598-022-26410-9 (2022).
23. Naik, B. et al. Pullulanase: unleashing the power of enzyme with a promising future in the food industry. *Front Bioeng. Biotechnol.* **11**, 1139611. https://doi.org/10.3389/fbioe.2023.1139611 (2023).
24. Dutta, D. & Sit, N. Comprehensive review on developments in starch-based films along with active ingredients for sustainable food packaging. *Sustain. Chem. Pharm.* **39**, 101534. https://doi.org/10.1016/j.scp.2024.101534 (2024).
25. Surendhiran, D. et al. Smart packaging film prepared from subcritical water-modified oat starch and betalain of beetroot extract reinforced with cellulose nanofibrils. *Sustain. Chem. Pharm.* **36**, 101349. https://doi.org/10.1016/j.scp.2023.101349 (2023).
26. Kumar, S. R. et al. Effects of single and dual modifications with debranching and heat-moisture treatments on physicochemical, rheological, and digestibility properties of proso millet starch. *Carbohydr. Polym. Technol. Appl.* **6**, 100399. https://doi.org/10.1016/j.carpta.2023.100399 (2023).
27. Jafari, M. & Koocheki, A. Impact of ultrasound treatment on the physicochemical and rheological properties of acid hydrolyzed sorghum starch. *Int. J. Biol. Macromol.* **256**, 128521. https://doi.org/10.1016/j.ijbiomac.2023.128521 (2024).
28. Abedi, E., Roohi, R., Hashemi, S. M. B. & Kaveh, S. Investigation of ultrasound-assisted starch acetylation by single- and dual- frequency ultrasound based on rheology modelling, non-isothermal reaction kinetics, and flow/acoustic simulation. *Ultrason. Sonochem.* **102**, 106737. https://doi.org/10.1016/j.ultsonch.2023.106737 (2024).
29. Shen, H. et al. Dielectric barrier discharge plasma improved the fine structure, physicochemical properties and digestibility of α-amylase enzymatic wheat starch. *Innov. Food Sci. Emerg. Technol.* **78**, 102991. https://doi.org/10.1016/j.ifset.2022.102991 (2022).
30. Shi, M. -m & Gao, Q. -y Physicochemical properties, structure and in vitro digestion of resistant starch from waxy rice starch. *Carbohydr. Polym.* **84**, 1151–1157, https://doi.org/10.1016/j.carbpol.2011.01.004 (2011).
31. Tu, D. et al. Effects of freeze-thaw treatment and pullulanase debranching on the structural properties and digestibility of lotus seed starch-glycerin monostearin complexes. *Int. J. Biol. Macromol.* **177**, 447–454, https://doi.org/10.1016/j.ijbiomac.2021.02.168 (2021).
32. Shen, G. et al. Preparation of potato flour by freeze-thaw pretreatment: Effect of different thawing methods on hot-air drying process and physicochemical properties. *LWT* **133**, 110157. https://doi.org/10.1016/j.lwt.2020.110157 (2020).
33. Huang, P.-H., Wang, T.-S. & Chang, W.-C. Insights into the physicochemical and structural properties of pumpkin flour via

synergistic treatments with debranching enzymes and freeze-thaw cycle. *Food Hydrocoll.* **157**, 110421. https://doi.org/10.1016/j.foodhyd.2024.110421 (2024).
34. Tao, H. et al. A comparative study of sodium dodecyl sulfate and freezing/thawing treatment on wheat starch: The role of water absorption. *Carbohydr. Polym.* **143**, 149–154, https://doi.org/10.1016/j.carbpol.2016.02.014 (2016).
35. Wang, Y. et al. Sequential starch modification by branching enzyme and 4-α-glucanotransferase improves retention of curcumin in starch-alginate beads. *Carbohydr. Polym.* **323**, 121387. https://doi.org/10.1016/j.carbpol.2023.121387 (2024).
36. Zhang, B., Huang, Q., Luo, F. -x & Fu, X. Structural characterizations and digestibility of debranched high-amylose maize starch complexed with lauric acid. *Food Hydrocoll.* **28**, 174–181, https://doi.org/10.1016/j.foodhyd.2011.12.020 (2012).
37. Liu, G., Hong, Y., Gu, Z., Li, Z. & Cheng, L. Pullulanase hydrolysis behaviors and hydrogel properties of debranched starches from different sources. *Food Hydrocoll.* **45**, 351–360, https://doi.org/10.1016/j.foodhyd.2014.12.006 (2015).
38. Yan, Y. et al. Debranching facilitates malate esterification of waxy maize starch and decreases the digestibility. *Int. J. Biol. Macromol.* **242**, 125056. https://doi.org/10.1016/j.ijbiomac.2023.125056 (2023).
39. Zhu, L.-J., Liu, Q.-Q., Wilson, J. D., Gu, M.-H. & Shi, Y.-C. Digestibility and physicochemical properties of rice (Oryza sativa L.) flours and starches differing in amylose content. *Carbohydr. Polym.* **86**, 1751–1759, https://doi.org/10.1016/j.carbpol.2011.07.017 (2011).
40. Liu, W. et al. In structure and in-vitro digestibility of waxy corn starch debranched by pullulanase. *Food Hydrocoll.* **67**, 104–110, https://doi.org/10.1016/j.foodhyd.2016.12.036 (2017).
41. Dodi, R. et al. Effect of the pasta making process on slowly digestible starch content. *Foods* **12**, 2064, https://doi.org/10.3390/foods12102064 (2023).
42. Guo, J., Gutierrez, A., Tan, L. & Kong, L. Considerations and strategies for optimizing health benefits of resistant starch. *Curr. Opin. Food Sci.* **51**, 101008. https://doi.org/10.1016/j.cofs.2023.101008 (2023).
43. Di Pede, G. et al. Glycemic Index values of pasta products: An overview. *Foods* **10**, 2541, https://doi.org/10.3390/foods10112541 (2021).
44. Li, C. Recent progress in understanding starch gelatinization - An important property determining food quality. *Carbohydr. Polym.* **293**, 119735. https://doi.org/10.1016/j.carbpol.2022.119735 (2022).
45. Cousin, M., Cuzon, G., Guillaume, J. & Aquacop Digestibility of starch in Penaeus vannamei: in vivo and in vitro study on eight samples of various origin. *Aquaculture* **140**, 361–372, https://doi.org/10.1016/0044-8486(95)01201-X (1996).
46. Miao, M., Jiang, B. & Zhang, T. Effect of pullulanase debranching and recrystallization on structure and digestibility of waxy maize starch. *Carbohydr. Polym.* **76**, 214–221, https://doi.org/10.1016/j.carbpol.2008.10.007 (2009).
47. Ou, Y. et al. Effects of exogenous V-type complexes on the structural properties and digestibility of autoclaved lotus seed starch after retrogradation. *Int. J. Biol. Macromol.* **165**, 231–238, https://doi.org/10.1016/j.ijbiomac.2020.09.153 (2020).
48. Kotatha, D., Wandee, Y., Udchumpisai, W. & Pattarapanawan, M. Fortification of dietary fiber in cassava pulp by conversion of the remaining starch to resistant starch. *Future Foods* **8**, 100265. https://doi.org/10.1016/j.fufo.2023.100265 (2023).
49. Gutiérrez, T. J. & Tovar, J. Update of the concept of type 5 resistant starch (RS5): Self-assembled starch V-type complexes. *Trends Food Sci. Technol.* **109**, 711–724, https://doi.org/10.1016/j.tifs.2021.01.078 (2021).
50. Guo, J. & Kong, L. Inhibition of in vitro starch digestion by ascorbyl palmitate and its inclusion complex with starch. *Food Hydrocoll.* **121**, 107032. https://doi.org/10.1016/j.foodhyd.2021.107032 (2021).
51. Lopez-Rubio, A., Flanagan, B. M., Shrestha, A. K., Gidley, M. J. & Gilbert, E. P. Molecular rearrangement of starch during in vitro digestion: toward a better understanding of enzyme resistant starch formation in processed starches. *Biomacromolecules* **9**, 1951–1958, https://doi.org/10.1021/bm800213h (2008).
52. Pongjanta, J., Utaipattanaceep, A., Naivikul, O. & Piyachomkwan, K. Debranching enzyme concentration effected on physicochemical properties and α-amylase hydrolysis rate of resistant starch type III from amylose rice starch. *Carbohydr. Polym.* **78**, 5–9, https://doi.org/10.1016/j.carbpol.2009.03.037 (2009).
53. Gidley, M. J. & Bulpin, P. V. Crystallisation of malto-oligosaccharides as models of the crystalline forms of starch: minimum chain-length requirement for the formation of double helices. *Carbohydr. Res.* **161**, 291–300, https://doi.org/10.1016/S0008-6215(00)90086-7 (1987).
54. Li, H. et al. In vitro digestibility of rice starch granules modified by β-amylase, transglucosidase and pullulanase. *Int. J. Biol. Macromol.* **136**, 1228–1236, https://doi.org/10.1016/j.ijbiomac.2019.06.111 (2019).
55. Zhang, S. et al. A- and B-type wheat starch granules: The multiscale structural evolution during digestion and the distinct digestion mechanisms. *Int. J. Biol. Macromol.* **278**, 135033. https://doi.org/10.1016/j.ijbiomac.2024.135033 (2024).
56. Wang, J., Huang, J., Liang, Q. & Gao, Q. Effects of heat–moisture treatment on structural characteristics and in vitro digestibility of A- and B-type wheat starch. *Int. J. Biol. Macromol.* **256**, 128012. https://doi.org/10.1016/j.ijbiomac.2023.128012 (2024).
57. Gunaratne, A. & Hoover, R. Effect of heat–moisture treatment on the structure and physicochemical properties of tuber and root starches. *Carbohydr. Polym.* **49**, 425–437, https://doi.org/10.1016/S0144-8617(01)00354-X (2002).
58. Geng, D.-H. et al. Structural, physicochemical and digestive properties of rice starch modified by preheating and pullulanase treatments. *Carbohydr. Polym.* **313**, 120866. https://doi.org/10.1016/j.carbpol.2023.120866 (2023).
59. Chakraborty, I. et al. An Insight into the gelatinization properties influencing the modified starches used in food industry: A review. *Food Bioprocess Technol.* **15**, 1195–1223, https://doi.org/10.1007/s11947-022-02761-z (2022).
60. Zhang, C., Lim, S.-T. & Chung, H.-J. Physical modification of potato starch using mild heating and freezing with minor addition of gums. *Food Hydrocoll.* **94**, 294–303, https://doi.org/10.1016/j.foodhyd.2019.03.027 (2019).
61. Piecyk, M. & Domian, K. Effects of heat–moisture treatment conditions on the physicochemical properties and digestibility of field bean starch (Vicia faba var. minor). *Int. J. Biol. Macromol.* **182**, 425–433, https://doi.org/10.1016/j.ijbiomac.2021.04.015 (2021).
62. Singh, N., Isono, N., Srichuwong, S., Noda, T. & Nishinari, K. Structural, thermal and viscoelastic properties of potato starches. *Food Hydrocoll.* **22**, 979–988, https://doi.org/10.1016/j.foodhyd.2007.05.010 (2008).
63. Wang, Q. et al. Physicochemical properties and nutritional quality of pre-fermented red bean steamed buns as affected by freeze-thaw cycling. *Int. J. Food Prop.* **25**, 748–763, https://doi.org/10.1080/10942912.2022.2060252 (2022).
64. Huang, H.-H. & Liao, H.-J. Digestion kinetics and molecular structural evolution during in vitro digestion of green banana (cv. Giant Cavendish) starch nanoparticles. *Food Res. Int.* **170**, 113016. https://doi.org/10.1016/j.foodres.2023.113016 (2023).
65. Low, Q. Y. & Liao, H.-J. Effects of incorporated emulsifiers into noodles on v-amylose formation, digestibility, and structural characteristics. *Plant Foods Hum. Nutr.* **78**, 604–612, https://doi.org/10.1007/s11130-023-01096-0 (2023).
66. Wongsagonsup, R., Varavinit, S. & BeMiller, J. N. Increasing slowly digestible starch content of normal and waxy maize starches and

properties of starch products. *Cereal Chem.* **85**, 738–745, https://doi.org/10.1094/CCHEM-85-6-0738 (2008).
67. Kong, L., Perez-Santos, D. M. & Ziegler, G. R. Effect of guest structure on amylose-guest inclusion complexation. *Food Hydrocoll.* **97**, 105188. https://doi.org/10.1016/j.foodhyd.2019.105188 (2019).
68. Hasjim, J. et al. Characterization of a novel resistant-starch and its effects on postprandial plasma-glucose and insulin responses. *Cereal Chem.* **87**, 257–262, https://doi.org/10.1094/CCHEM-87-4-0257 (2010).
69. Zheng, Y. et al. Effects of pullulanase pretreatment on the structural properties and digestibility of lotus seed starch-glycerin monostearin complexes. *Carbohydr. Polym.* **240**, 116324. https://doi.org/10.1016/j.carbpol.2020.116324 (2020).
70. Chen, B. et al. Slowly digestible properties of lotus seed starch-glycerine monostearin complexes formed by high pressure homogenization. *Food Chem.* **252**, 115–125, https://doi.org/10.1016/j.foodchem.2018.01.054 (2018).
71. Liu, X. et al. Changes of starch during thermal processing of foods: Current status and future directions. *Trends Food Sci. Technol.* **119**, 320–337, https://doi.org/10.1016/j.tifs.2021.12.011 (2022).
72. Reddy, C. K., Haripriya, S., Noor Mohamed, A. & Suriya, M. Preparation and characterization of resistant starch III from elephant foot yam (Amorphophallus paeonifolius) starch. *Food Chem.* **155**, 38–44, https://doi.org/10.1016/j.foodchem.2014.01.023 (2014).
73. Jia, R. et al. A review of starch swelling behavior: Its mechanism, determination methods, influencing factors, and influence on food quality. *Carbohydr. Polym.* **321**, 121260. https://doi.org/10.1016/j.carbpol.2023.121260 (2023).
74. Huang, P.-H., Cheng, Y.-T., Chan, Y.-J., Lu, W.-C. & Li, P.-H. Effect of cooking treatment on the formation mechanism and physicochemical properties of mung bean (Vigna radiata L.) paste. *J. Agric. Food Res.* **16**, 101054. https://doi.org/10.1016/j.jafr.2024.101054 (2024).
75. Liu, H. et al. Quality deterioration of frozen dough bread during terminal freezing and thawing: From the insight of moisture and starch properties. *Food Biosci.* **56**, 103435. https://doi.org/10.1016/j.fbio.2023.103435 (2023).
76. Guo, L., Deng, Y., Lu, L., Zou, F. & Cui, B. Synergistic effects of branching enzyme and transglucosidase on the modification of potato starch granules. *Int. J. Biol. Macromol.* **130**, 499–507, https://doi.org/10.1016/j.ijbiomac.2019.02.160 (2019).
77. Chang, Q., Zheng, B., Zhang, Y. & Zeng, H. A comprehensive review of the factors influencing the formation of retrograded starch. *Int. J. Biol. Macromol.* **186**, 163–173, https://doi.org/10.1016/j.ijbiomac.2021.07.050 (2021).
78. Zhang, W., Bao, Y. & Li, H.-T. Altering structure and enzymatic resistance of high-amylose maize starch by irradiative depolymerization and annealing with palmitic acid as V-type inclusion compound. *Carbohydr. Polym.* **322**, 121343. https://doi.org/10.1016/j.carbpol.2023.121343 (2023).
79. Wang, D. et al. Preparation and characterization of debranched starches: Influence of botanical source and debranching time. *Food Chem.* **407**, 135141. https://doi.org/10.1016/j.foodchem.2022.135141 (2023).
80. Wang, D. et al. Effect of modification by maltogenic amylase and branching enzyme on the structural and physicochemical properties of sweet potato starch. *Int. J. Biol. Macromol.* **239**, 124234. https://doi.org/10.1016/j.ijbiomac.2023.124234 (2023).
81. Bao, J., Zhou, X., Hu, Y. & Zhang, Z. Resistant starch content and physicochemical properties of non-waxy rice starches modified by pullulanase, heat-moisture treatment, and citric acid. *J. Cereal Sci.* **105**, 103472. https://doi.org/10.1016/j.jcs.2022.103472 (2022).
82. Guo, J., Ellis, A., Zhang, Y., Kong, L. & Tan, L. Starch-ascorbyl palmitate inclusion complex, a type 5 resistant starch, reduced in vitro digestibility and improved in vivo glycemic response in mice. *Carbohydr. Polym.* **321**, 121289. https://doi.org/10.1016/j.carbpol.2023.121289 (2023).
83. Tan, L. & Kong, L. Starch-guest inclusion complexes: Formation, structure, and enzymatic digestion. *Crit. Rev. Food Sci. Nutr.* **60**, 780–790, https://doi.org/10.1080/10408398.2018.1550739 (2020).
84. Thérien-Aubin, H. & Zhu, X. X. NMR spectroscopy and imaging studies of pharmaceutical tablets made of starch. *Carbohydr. Polym.* **75**, 369–379, https://doi.org/10.1016/j.carbpol.2008.08.010 (2009).
85. Niu, B. et al. Effect of plasma-activated water on the formation of endogenous wheat starch-lipid complexes during extrusion. *Int. J. Biol. Macromol.* **257**, 128647. https://doi.org/10.1016/j.ijbiomac.2023.128647 (2024).
86. Sherin, A. J., Sunil, C. K., Chidanand, D. V. & Venkatachalapathy, N. Structural, physicochemical and functional properties of high-pressure modified white finger millet starch. *Int. J. Biol. Macromol.* **261**, 129919. https://doi.org/10.1016/j.ijbiomac.2024.129919 (2024).
87. Li, H. et al. Modification of rice starch using a combination of autoclaving and triple enzyme treatment: Structural, physicochemical and digestibility properties. *Int. J. Biol. Macromol.* **144**, 500–508, https://doi.org/10.1016/j.ijbiomac.2019.12.112 (2020).
88. Li, W. et al. High pressure induced gelatinization of red adzuki bean starch and its effects on starch physicochemical and structural properties. *Food Hydrocoll.* **45**, 132–139, https://doi.org/10.1016/j.foodhyd.2014.11.013 (2015).
89. Jing, L. et al. Effect of repeated freezing-thawing on structural, physicochemical and digestible properties of normal and waxy starch gels. *Int. J. Food Sci. Technol.* **54**, 2668–2678, https://doi.org/10.1111/ijfs.14177 (2019).
90. Salari-Moghaddam, A., Saneei, P., Larijani, B. & Esmaillzadeh, A. Glycemic index, glycemic load, and depression: a systematic review and meta-analysis. *Eur. J. Clin. Nutr.* **73**, 356–365, https://doi.org/10.1038/s41430-018-0258-z (2019).
91. Li, P.-H., Wang, C.-W., Lu, W.-C., Chan, Y.-J. & Wang, C.-C. R. Effect of resistant starch sources on the physical properties of dough and on the eating quality and glycemic index of salted noodles. *Foods* **11**, 814, https://doi.org/10.3390/foods11060814 (2022).
92. Zhang, H., Sun, S. & Ai, L. Physical barrier effects of dietary fibers on lowering starch digestibility. *Curr. Opin. Food Sci.* **48**, 100940. https://doi.org/10.1016/j.cofs.2022.100940 (2022).
93. Ren, X. et al. In vitro starch digestibility and in vivo glycemic response of foxtail millet and its products. *Food Funct.* **7**, 372–379, https://doi.org/10.1039/C5FO01074H (2016).
94. Li, C. & Hu, Y. In vitro and animal models to predict the glycemic index value of carbohydrate-containing foods. *Trends Food Sci. Technol.* **120**, 16–24, https://doi.org/10.1016/j.tifs.2021.12.031 (2022).
95. Lin, Y.-W., Tsai, C.-L., Chen, C.-J., Li, P.-L. & Huang, P.-H. Insights into the effects of multiple frequency ultrasound combined with acid treatments on the physicochemical and thermal properties of brown rice postcooking. *LWT*, 115423. https://doi.org/10.1016/j.lwt.2023.115423
96. Huang, P.-H., Chiu, C.-S., Lu, W.-C. & Li, P.-H. Effect of compositions on physicochemical properties and rheological behavior of gelatinized adzuki-bean cake (Yokan). *LWT* **168**, 113870. https://doi.org/10.1016/j.lwt.2022.113870 (2022).
97. Huang, P.-H. et al. Response Surface Analysis and process optimisation of adzuki bean (Vigna angularis) food paste production. *J. Agric. Food Res.* **14**, 100855. https://doi.org/10.1016/j.jafr.2023.100855 (2023).
98. Cheng, Y.-T. et al. Investigate the composition and physicochemical properties attributes of banana starch and flour during ripening. *Carbohydrate Polymer Technologies and Applications*, 100446. https://doi.org/10.1016/j.carpta.2024.100446.

Acknowledgements
This research was financially supported by Taichung Veterans General Hospital and by Rong Sing Medical Foundation, Taiwan. This research was also supported by grants provided by the National Science and Technology Council (NSTC 114-2622-B-126 -001 -) in Taiwan.

Author contributions
Po-Yuan Chiang; Po-Hsien Li: Conceptualization, investigation, writing – original draft, visualization; Po-Hsien Li; Ping-Hsiu Huang: Writing – reviewing & editing, supervision; Yu-Tsung Cheng: Methodology, resources, reviewing; Wen-Chien Lu: Investigation, resources; Chin-Chuan Hsu; Chiun-Chuang R. Wang: Methodology, resources, project administration.

Competing interests
The authors declare no competing interests.

Additional information
Supplementary information The online version contains supplementary material available at https://doi.org/10.1038/s41538-025-00603-8.

Correspondence and requests for materials should be addressed to Po-Hsien Li.